SOFT X-RAY TELESCOPE AND ITS CAPABILITIES

K. P. Singh
IISER- Mohali, TIFR Mumbai

@AADA Workshop, IUCAA, June 23, 2021

AstroSat in a clean room before Launch

SXT: India’s first Soft X-ray focusing Telescope (~65 Kg)

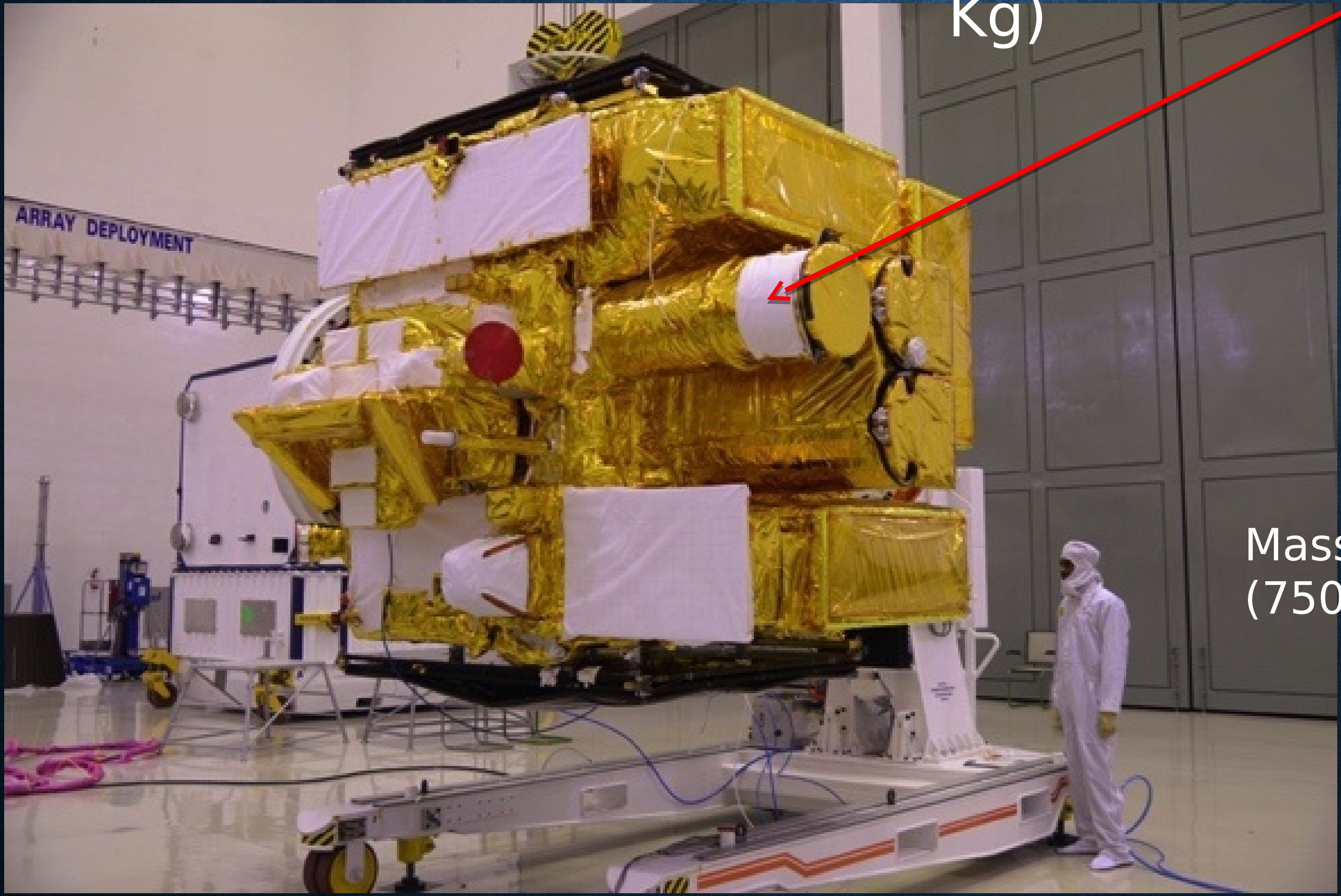

Mass of 1513 kg.
(750 kg. Payloads)

SXT: OPTICS + CCD BASED FPCA

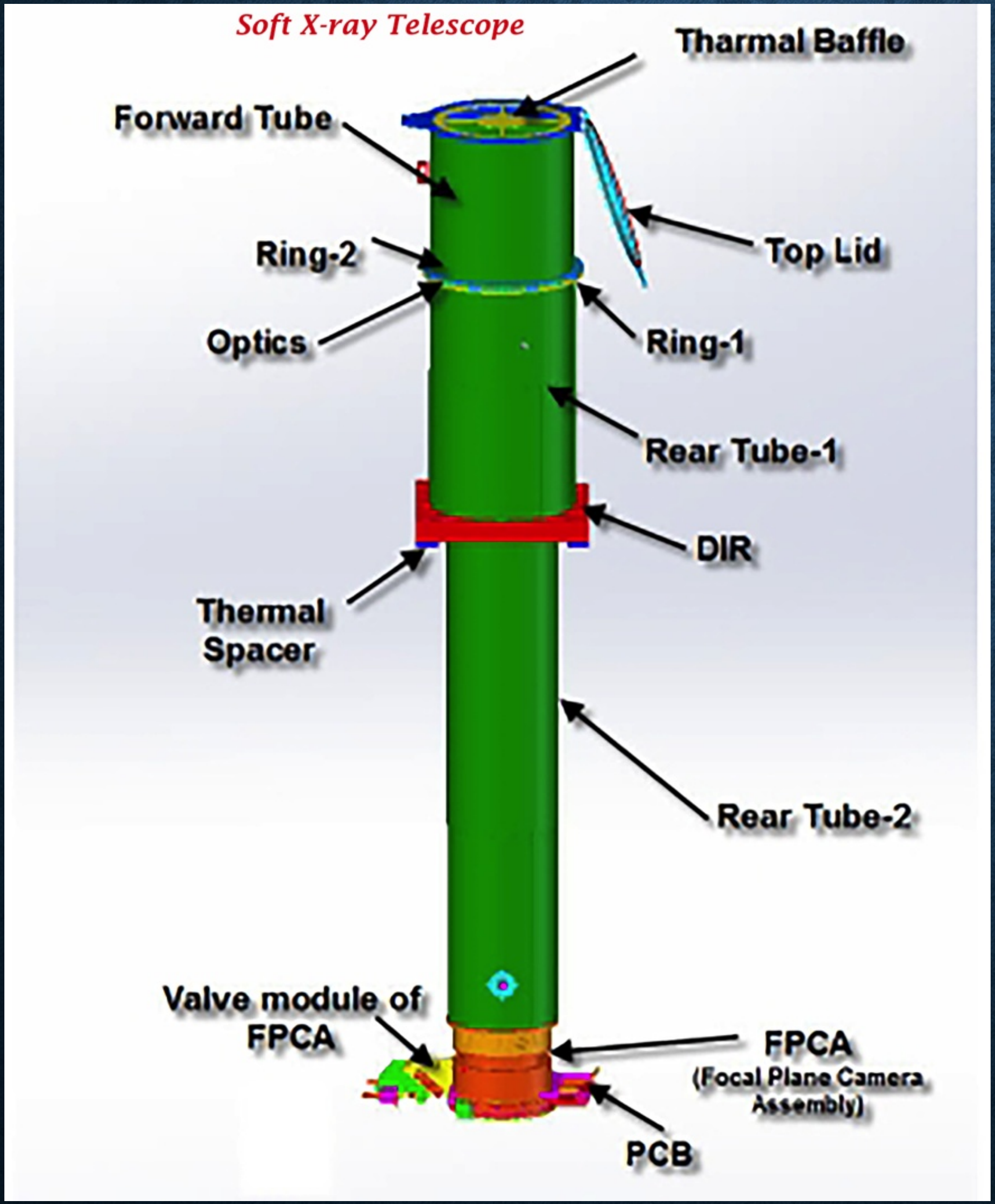

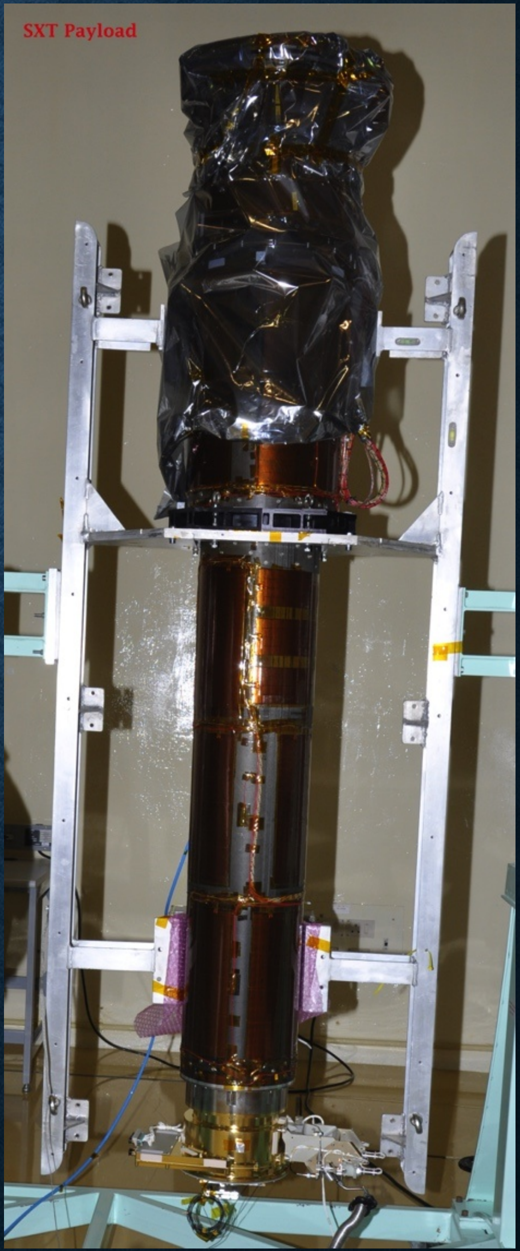

KPSingh

WHY DO WE USE X-RAY FOCUSING?

- To achieve 2-dimensional angular resolution to get *Accurate positions specially in crowded regions, image different parts of the same source for morphology*
- To collect or "gather" weak fluxes of photons – from faint and distant sources
- To concentrate/focus, so that the photons interact in a small region of the detector thus making non-X-ray background almost negligible
- To serve with high spectral resolution dispersive spectrometers such as transmission or reflection gratings
- To simultaneously measure both the sources of interest, and the contaminating background using other regions of the detector.

X-RAY OPTICS:
BASIC REQUIREMENTS

We must make the X-rays Reflect

- Total External Reflection

We must make the X-rays focus & form an Image

- Control Mirror Figure
- Control Scattering

Refractive Index for X-rays incident on a metal surface

- X-rays incident on a metal surface see most electrons as free

- Electron number density of plasma of electrons in a metal seen by the incident X-rays is

$$N_e = (Z\text{-}2)\rho/Am_p \ \text{electrons/cm}^3$$

- Refractive Index of the plasma,

$$n = (1 - \omega_p^2/\omega^2)^{1/2} \text{ , where}$$

$$\omega_p = 4\pi N_e e^2/m_e \text{ is the "plasma frequency"}$$

- n < 1 for X-rays ($\omega > \omega_p$) in a metal

SNELL'S LAW AND TOTAL EXTERNAL REFLECTION

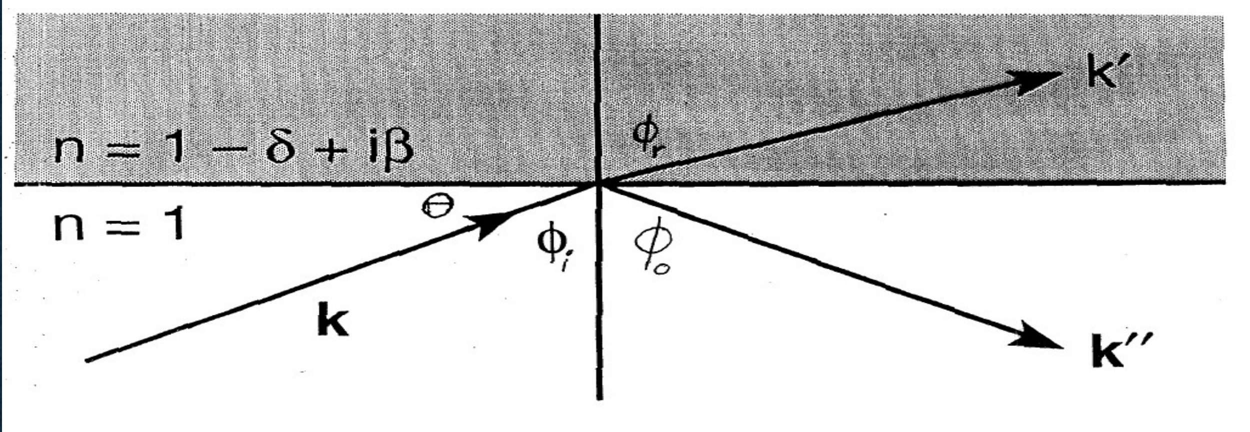

- Snell's law for refraction, ***$\sin\phi_i = n \sin \phi_r$***

where ϕ is the standard angle of incidence from the surface normal, θ is the grazing angle from the surface.

- Since n < 1 for X-rays in a metal, X-rays bend away from the normal and most are absorbed
- When ϕ_i approaches 90^o=X-rays undergo total internal ("external") reflection and we can write in terms of critical angle of reflection from the surface, $\cos \theta = (1 - \omega_p^2/\omega^2)^{1/2}$

CRITICAL GRAZING ANGLE

Using Taylor Series expansion on both sides

$1 - \theta^2/2 = 1 - 0.5\, \omega_p{}^2/\omega^2 \quad \rightarrow$

$\theta = \omega_p/\omega$ using $\omega = 2\pi c/\lambda$

$\theta = [(Z-2)\rho\, \lambda^2\, N\, e^2\ / (A\, m_e\, \pi\, c)]^{1/2}$

Therefore θ is proportional to $(Z)^{1/2}/E$

- The critical angle decreases inversely proportional to the energy.
- Higher Z materials reflect higher energies, for fixed grazing angles.
- Higher Z materials have a larger critical angle at any energy.

For heavy elements, Ni, Au, Pt, Ir, etc. Z / A = 0.5, and

$\theta = 5.6\, \lambda\, \rho^{1/2}$ arcmin

(λ is in Angstroms, and ρ is in gm/cm^3) < 1 deg.

X-RAY REFLECTIVITY OF METALS

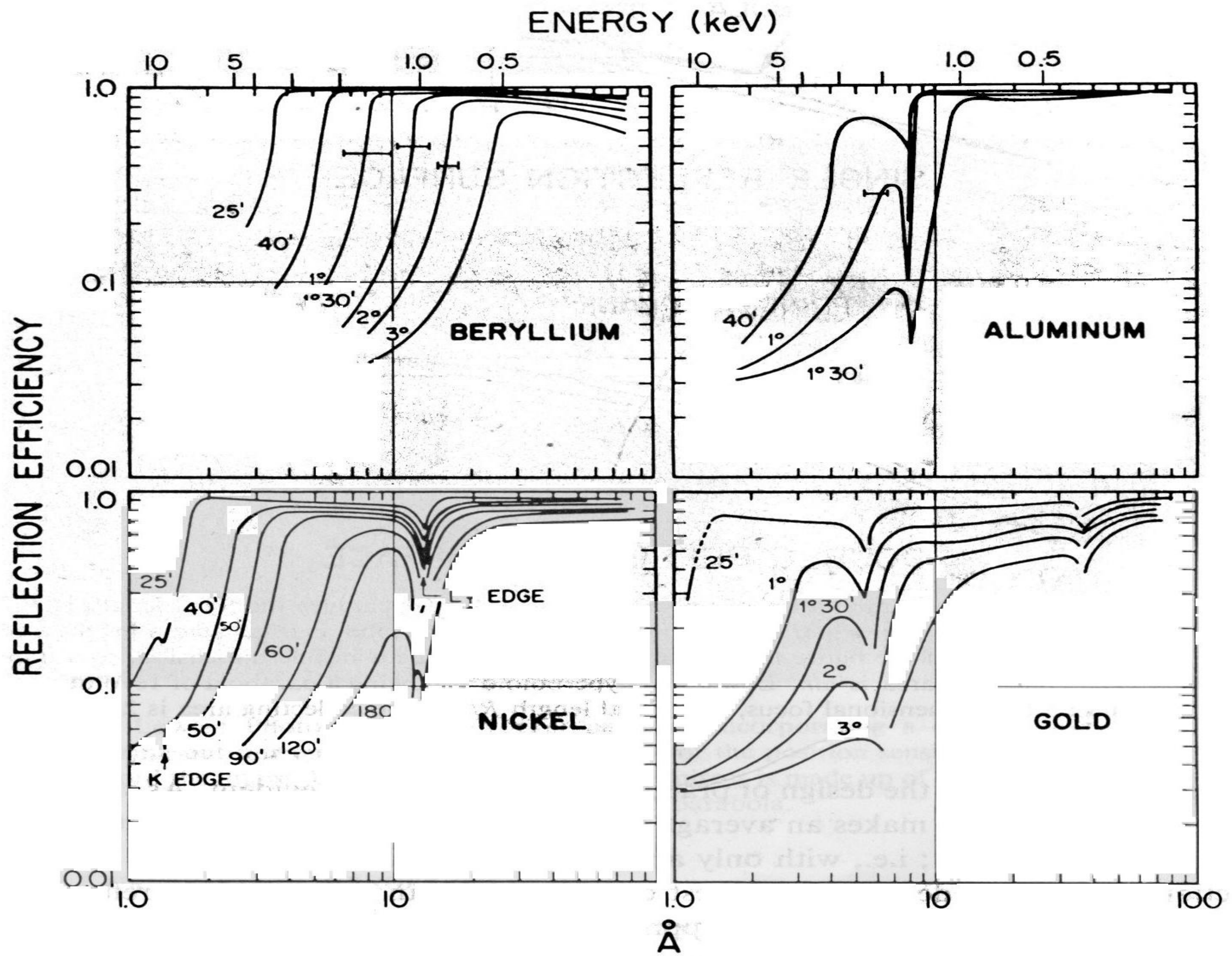

Fig. 2.20 Theoretical reflection efficiencies of Be($Z=4$), Al($Z=13$), Ni($Z=28$), and Au($Z=79$) surfaces as a function of energy or wavelength, for various grazing angles. Actual mirrors are less efficient, depending sensitively on the surface finish. The critical angle for a given energy may be defined as the angle at which the reflectivity drops below some arbitrary level, e.g. 10 %. The complexities of the curves are due to absorption edge effects.

X-RAY REFLECTION: NOT THE END OF THE STORY

- Some Significant effects remain:

The surfaces are not infinitely smooth.

This gives rise to the complex subject of X-ray scattering. Scattering cannot be treated *exactly, one must consider a statistical description* of the surface roughness.

Key Features:

- Scattering increases as E^2
- In plane scattering dominates by factor $\mathbf{1/\sin\theta}$

WE GENERALLY DO NOT HAVE A PERFECT INTERFACE FROM A VACUUM TO AN INFINITELY THICK REFLECTING LAYER.

We must consider:

- The mirror substrate material; e.g., Zerodur for Chandra
- A thin binding layer, e.g., Chromium, to hold the heavy metallic coating to the glass
- The high Z metal coating; e.g., Iridium for Chandra
- An unwanted but inadvertent overcoat of molecular contaminants

Feature: Interference can cause oscillations in reflectivity.

PREPARATION OF COATING AFFECTS REFLECTIVITY THROUGH THE DEPENDENCE ON DENSITY.

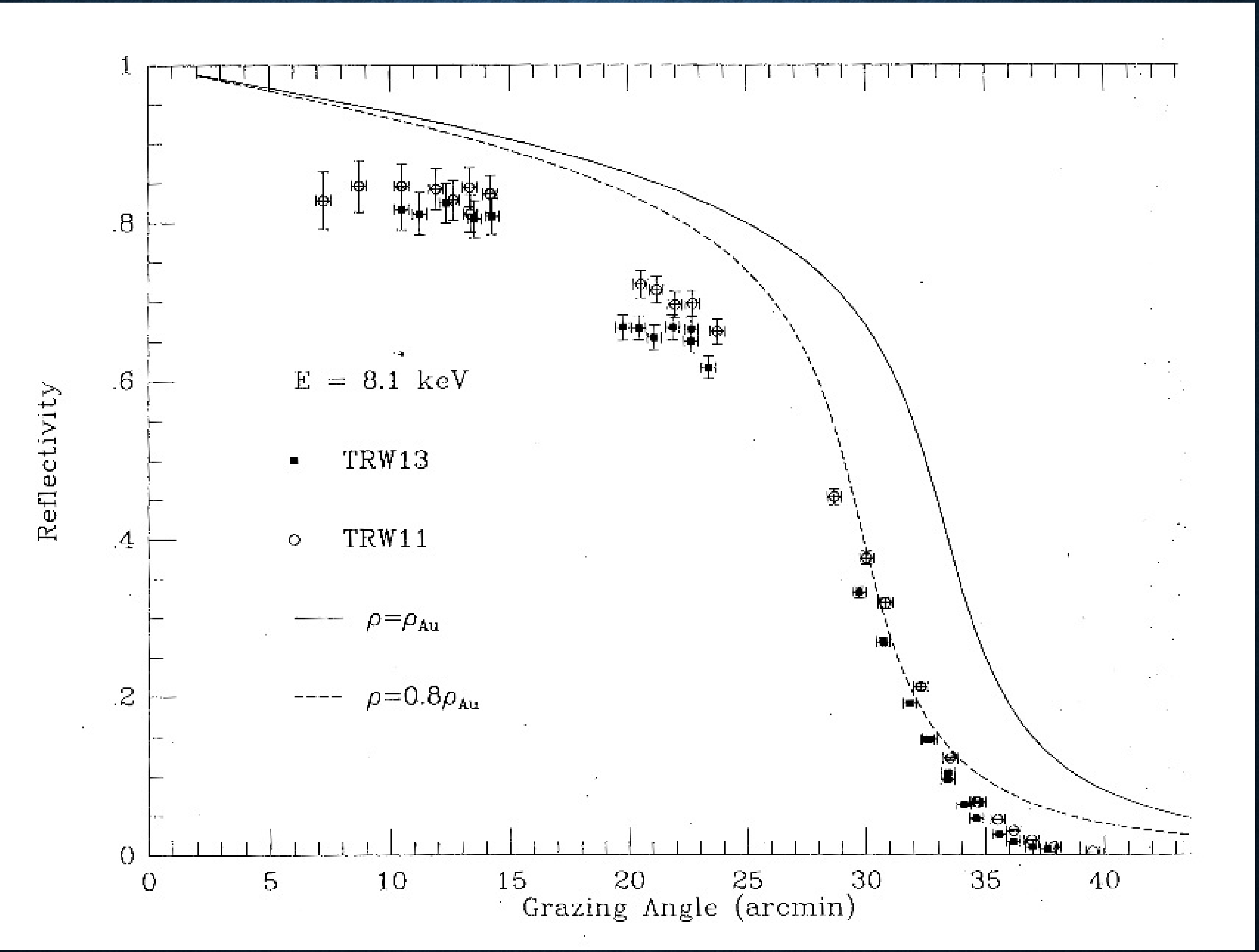

WOLTER'S CONFIGURATIONS

Wolter, H. 1952, *Ann. Physik 10, 94;ibid. 286;*
Giacconi, R. & Rossi, B. 1960, *J. Geophys. Res. 65, 773*

- A parabola of revolution (rotating the parabola around its central axis) will focus only the on-axis rays. Off-axis rays (off-axis by angle d will focus on a ring of radius Fd.
- A Paraboloid produces a perfect focus for on-axis rays.
- Off-axis it gives a coma blur size proportional to the distance off-axis.
- Wolter's classic paper proved two reflections were needed, and considered configurations of conics to eliminate coma.
- Basic Principle: The optical path to the image must be identical for all rays incident on the telescope, in order to achieve perfect imaging.
- Wolter derived three possible Geometries.

WOLTER'S CONFIGURATIONS

Wolter (1952) Ann. Phys., NY, 10, 94 & 286

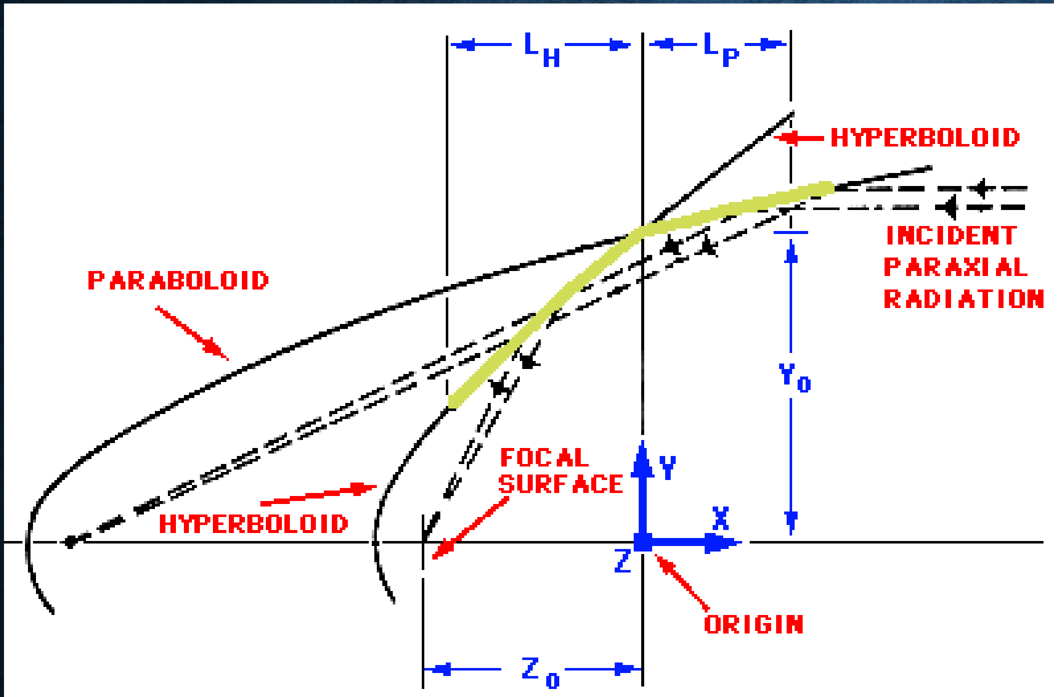

Type I

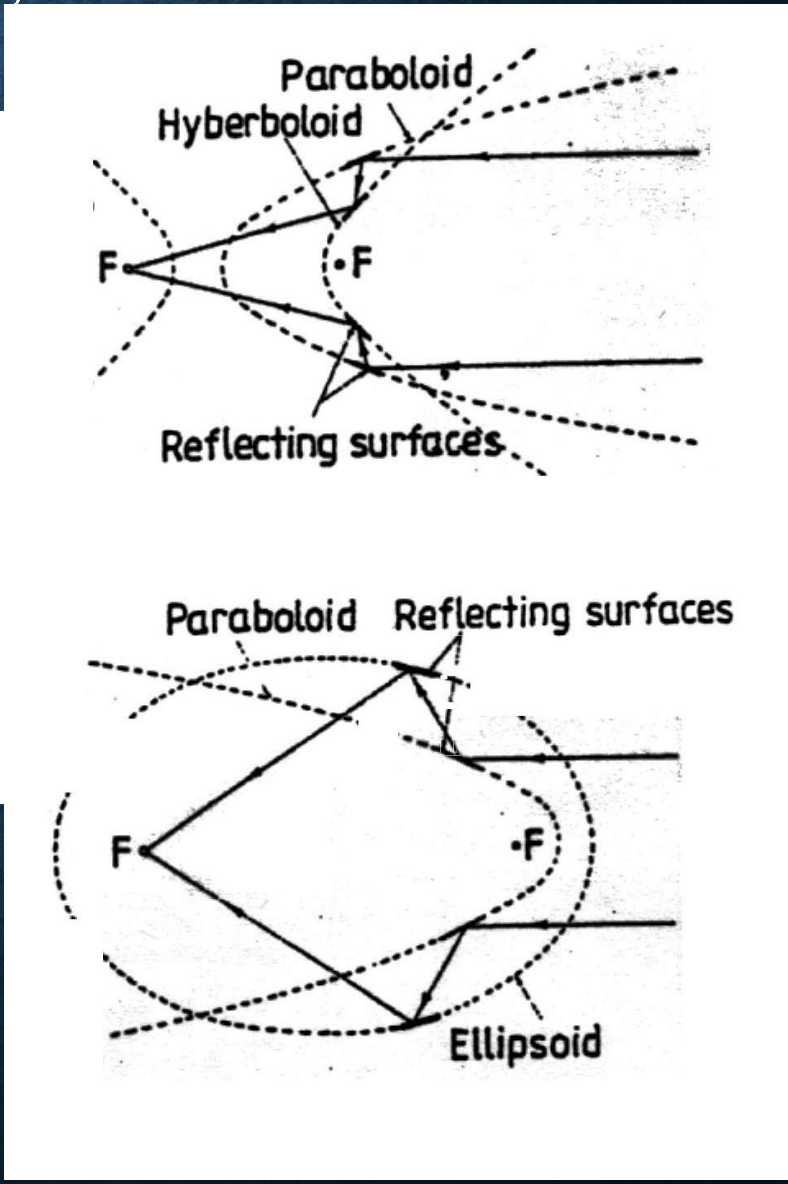

KPSingh

Types II, III

WOLTER-I CONFIGURATION

The Type I or the Paraboloid-Hyperboloid is overwhelmingly most useful in cosmic X-ray astronomy:

- Shortest Focal length to aperture ratio. This has been a key discriminator as we are always trying to maximize the collecting area to detect weak fluxes, but with relatively severe restrictions on length (and diameter) imposed by available space vehicles.
- For resolved sources, the shorter focal length concentrates a given spatial element of surface brightness onto a smaller detector area, hence gives a better signal to noise ratio against the non-X-ray detector background.

X-Ray Mirrors: Paraboloid-Hyperboloid

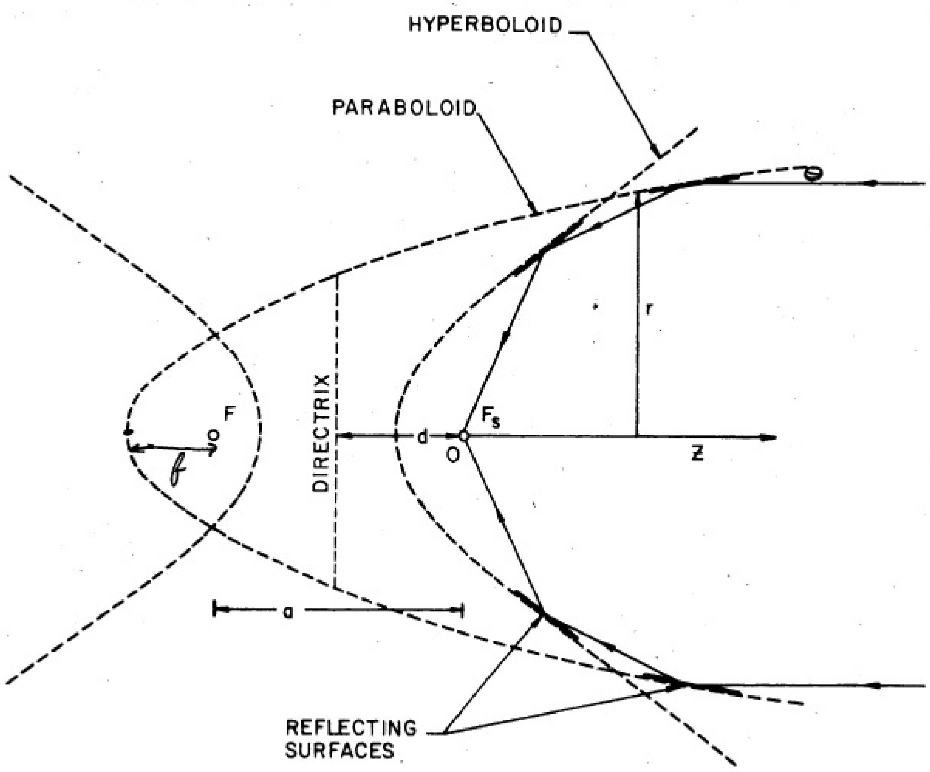

FIGURE 3 THE PRINCIPLE OF THE WOLTER TYPE I TELESCOPE. THE TELESCOPE FOCUS IS AT F_S. THE FOCUS OF THE PARABOLOID IS AT THE SECOND FOCUS OF THE HYPERBOLOID.

Advantages of intersecting P and H surfaces: mounting, nesting, and vignetting considerations. For replicated mirrors, the P and H figures are typically polished on a single mandrel and the pair formed as a single piece.

One requirement of the shorter focal length is that it puts more demand on having a detector with smaller spatial resolution in order to sample the image.

CHANDRA'S 4 NESTED X-RAY TELESCOPES

Increasing the Collecting area

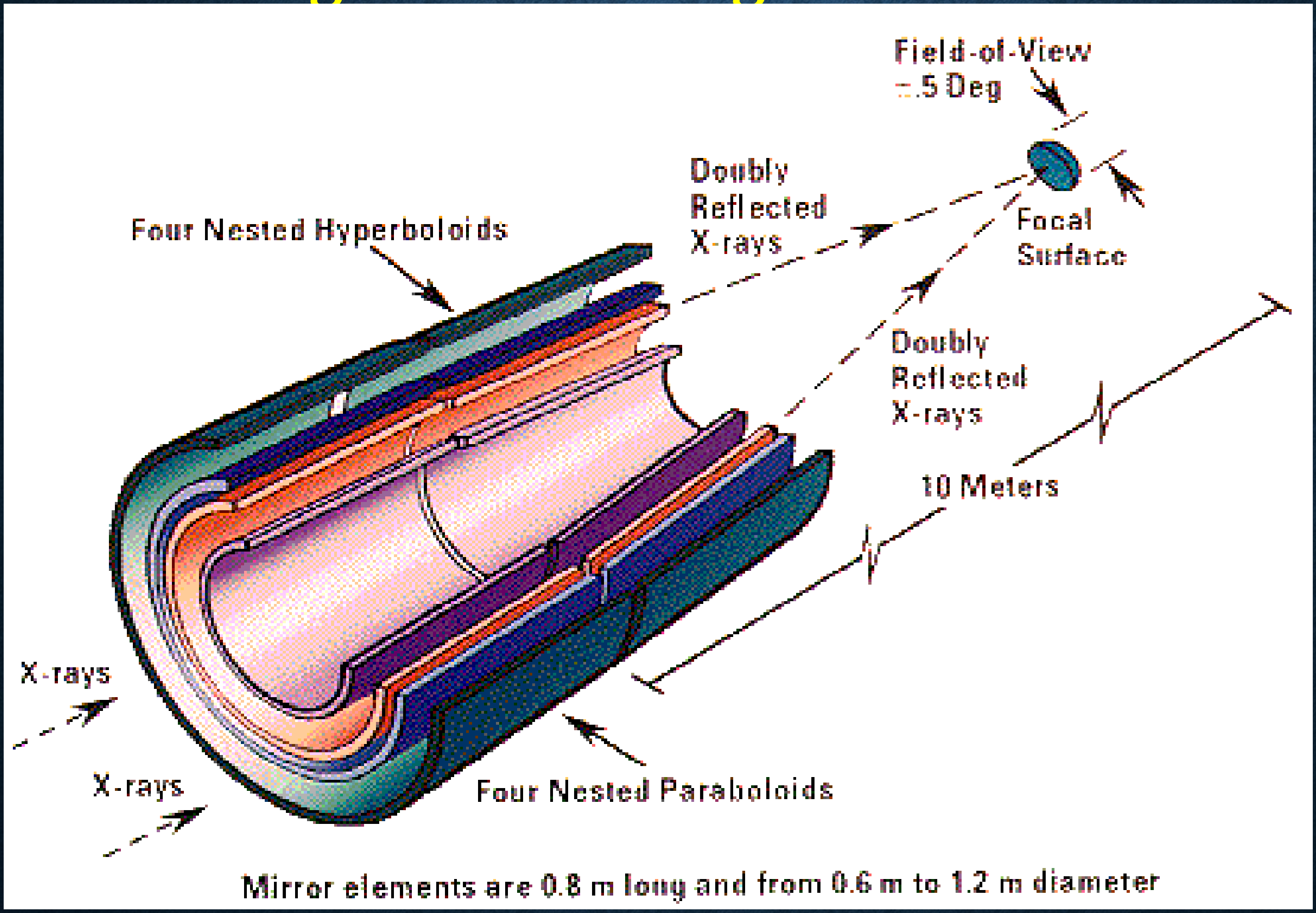

Launched: 23.7.1999

84 cm long mirrors; 10 m focal length; 1484 Kgs (mirrors only);

Area =1145 cm^2 (Geom.) and 0.5 arcsec resolution

X-RAY MULTI MIRROR (XMM)-NEWTON

Wolter Type 1 with 58 mirror shells of Nickel coated with Gold.
Focal Length: 750 cm
Outermost Mirror Dia:70cm
Innermost Mirror Dia:31.8cm
Axial Mirror Length paraboloid + hyperboloid: 60 cm
Wall Thickness: 1.07-0.47 mm
Min. Packing Distance: 3 mm
Mirror Module Mass: 437 kg
Angular Resolution, Half Energy Width 15 arc seconds, 0.1-10 keV

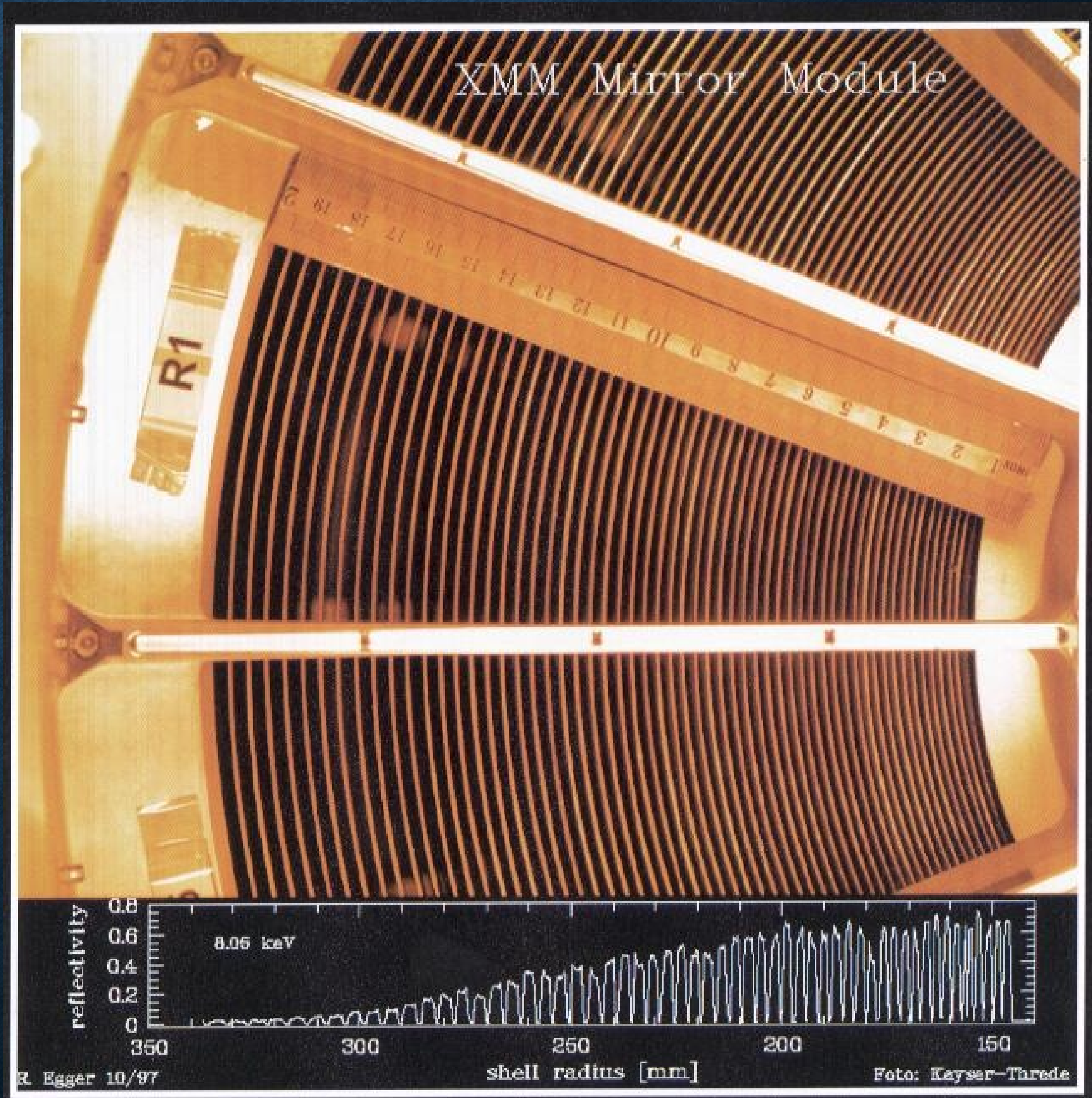

EPOXY REPLICATION PROCESS FOR FLAT FOILS

Conical Approximation to Wolter I:
Used for making Suzaku mirrors and adopted for a soft X-ray telescope for AstroSat

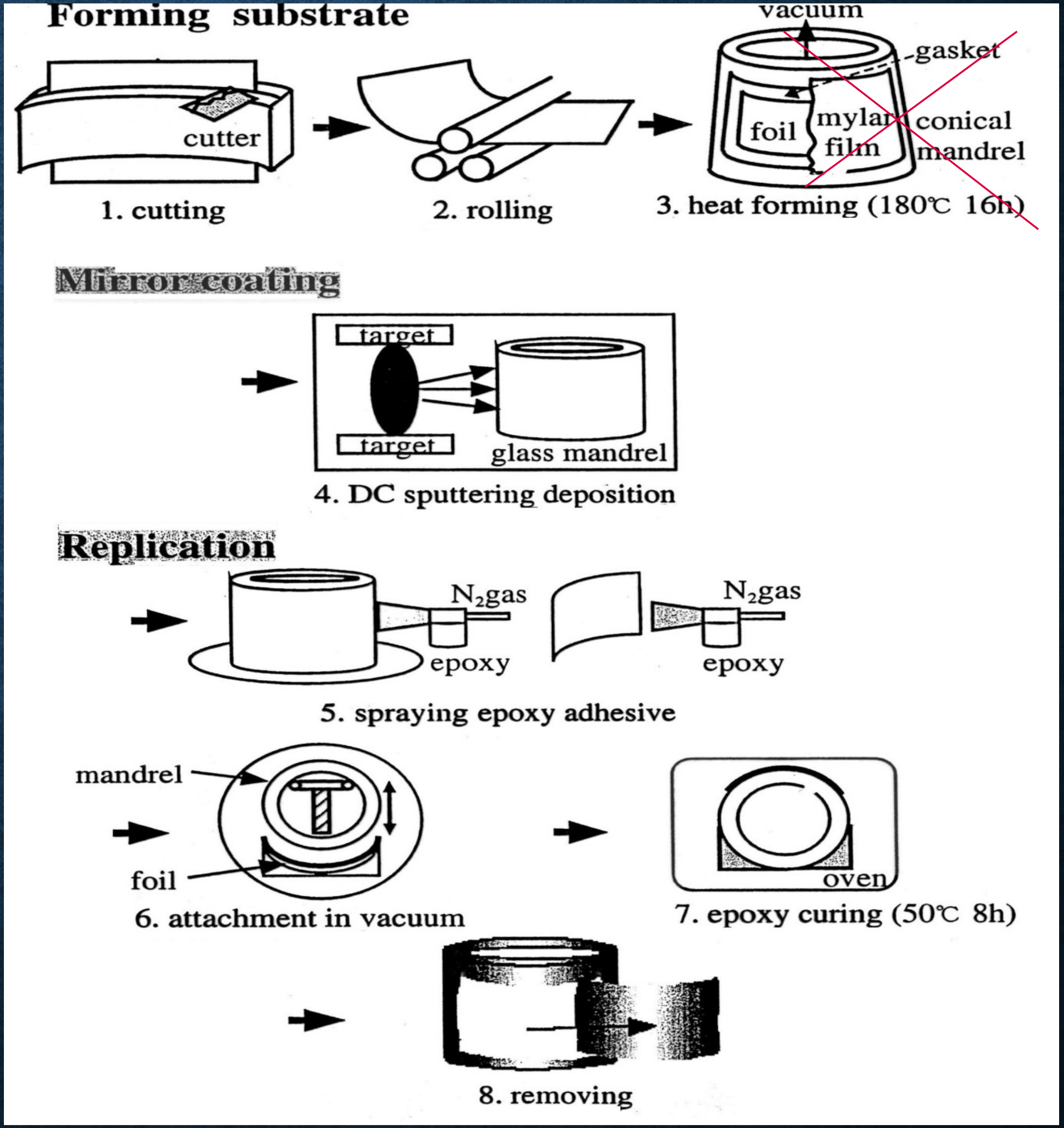

KPSingh

COMPARING TWO TYPES OF XRTS

Wolter-1 Optics vs.	**Conical Approx. Optics**
Exact machining of surface shapes	Approximate surfaces - easier to fabricate
Stiff and thick surfaces with low thermal expansion	Thin surfaces of metals (ready foils-replication)
Very poor nesting of many surfaces	Very high nesting possible
Small effective area	Larger effective area for same aperture
Limited high energy response or very large F.L. (8 - 10m)	Much better high energy response for same F.L.
Higher Angular resolution (arcsec)	Poorer angular resolution (arcmin)
Expensive Technology	Relatively much cheaper
Heavy (~ tonne)	Lighter (10 - 30 Kg.)
Einstein, ROSAT, Chandra	ASCA, Suzaku, AstroSat-SXT

X-ray Ground calibration: SXT Mirrors

Performance of SXT grazing incidence foil mirrors evaluated using Indus-1 soft x-ray reflectivity beamline

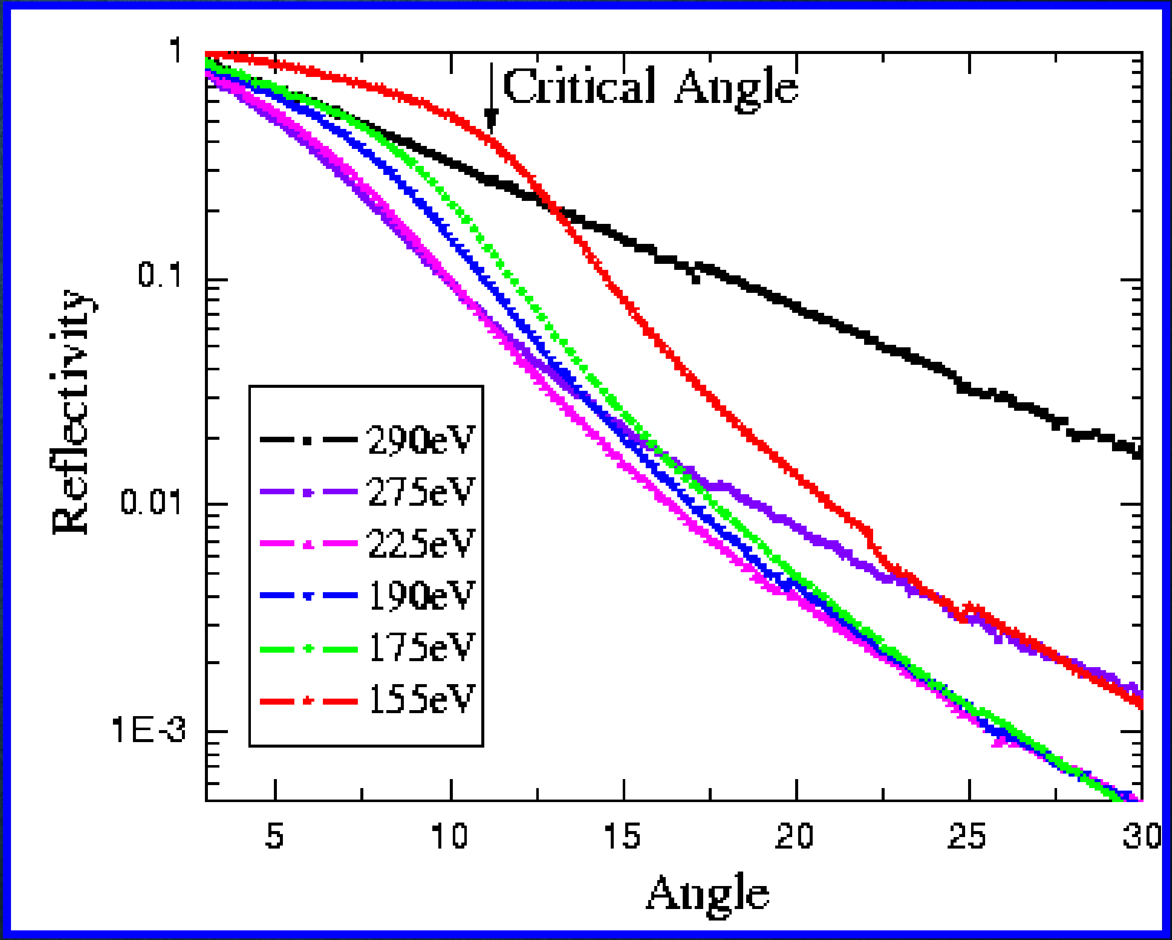

Archana et al Experimental Astronomy (2010)

X-ray Ground calibration

Performance of SXT grazing incidence foil mirrors evaluated at 5.4 and 8 keV.

Smoothness derived to be ~ 10 Angstroms

Surface layers are smoother than the deeper layers

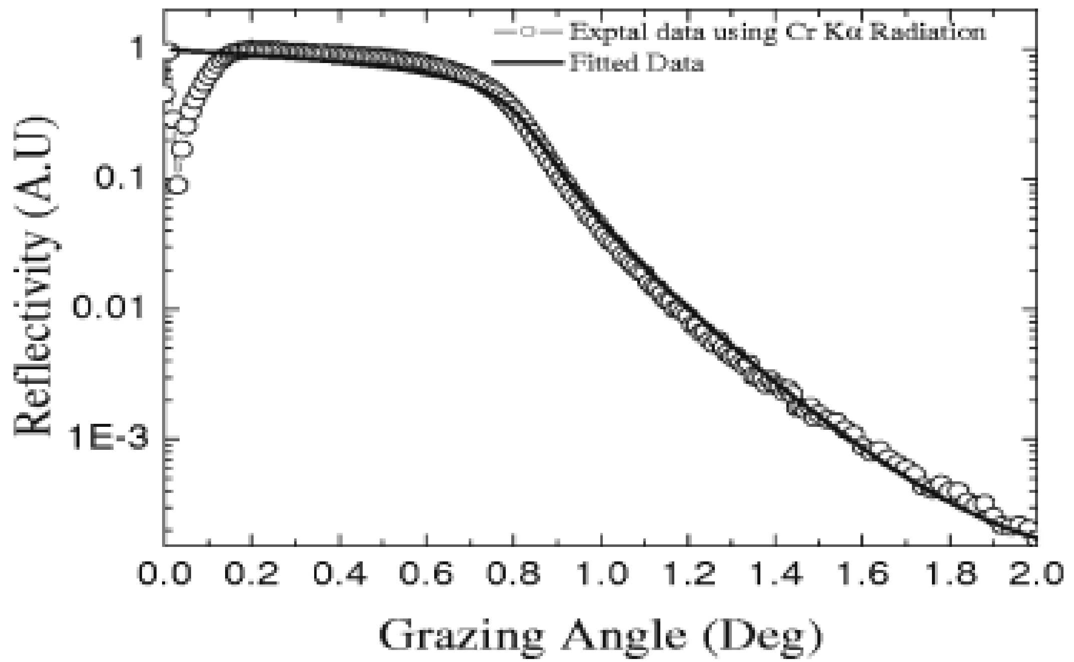

Fig. 6 X-ray reflectivity pattern obtained using Cr K_α X-rays for a typical sample of gold mirror

Archana et al Experimental Astronomy (2010)

ASTROSAT SXT: MIRRORS ASSEMBLY

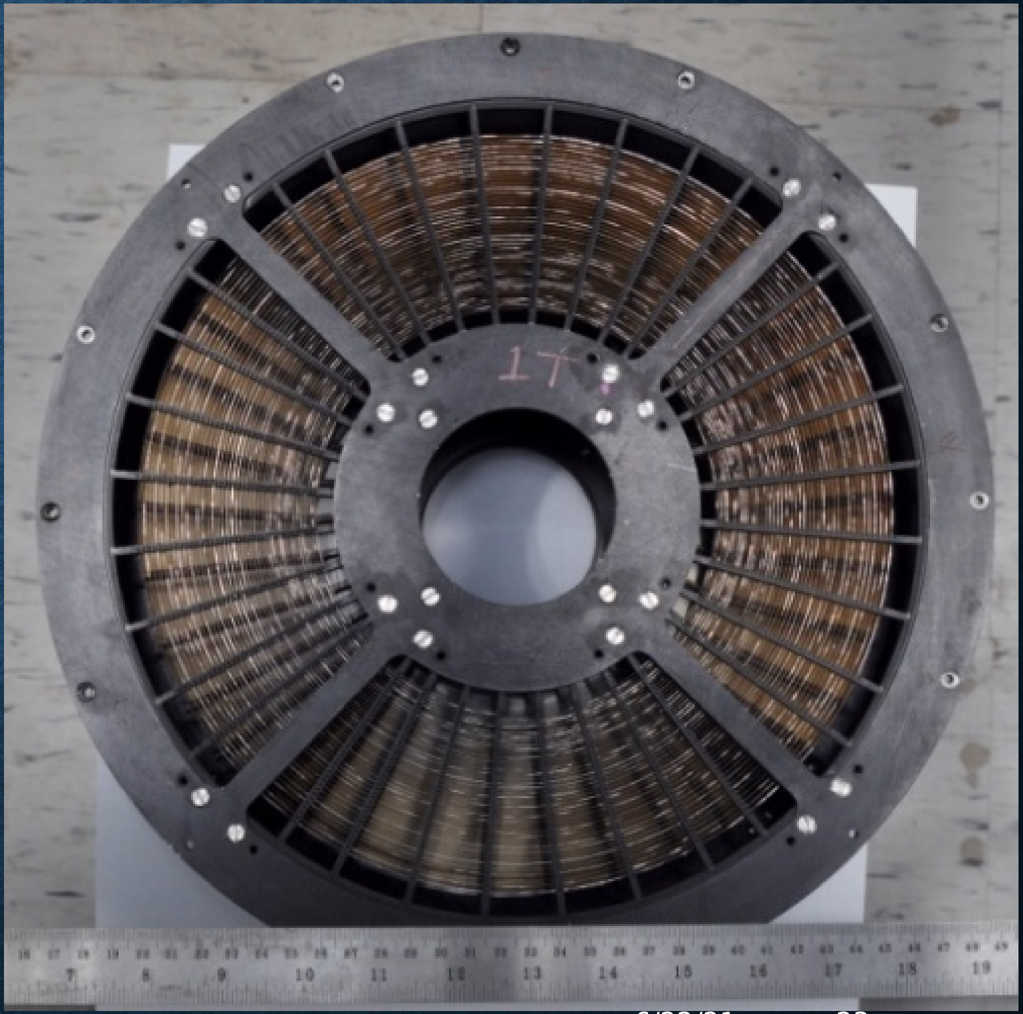

Number of nested shells = 40

SOFT X-RAY TELESCOPE

Telescope Length: 2460 mm
(Telescope + camera + baffle + door)
Top Envelope Diameter: 386 mm
Focal Length: 2000 mm
Maximum radius of foils: 130 mm
Minimum radius of foils: 65 mm
Reflector Length: 100 mm
Reflector thickness: 0.2 mm (Al) + Epoxy (50-60 microns) + gold 1400 Angstroms
Minimum reflector spacing: 0.5 mm
No. of reflectors: 320

ASTROSAT SXT: FM

- Characterization and proof of assembly thru Optical laser beam tests of all individual mirrors (320) and full beam. Depth of focus checked – no change up to 3-4 mm

Full aperture optical light test to check the FM SXT optics at 2m focal length

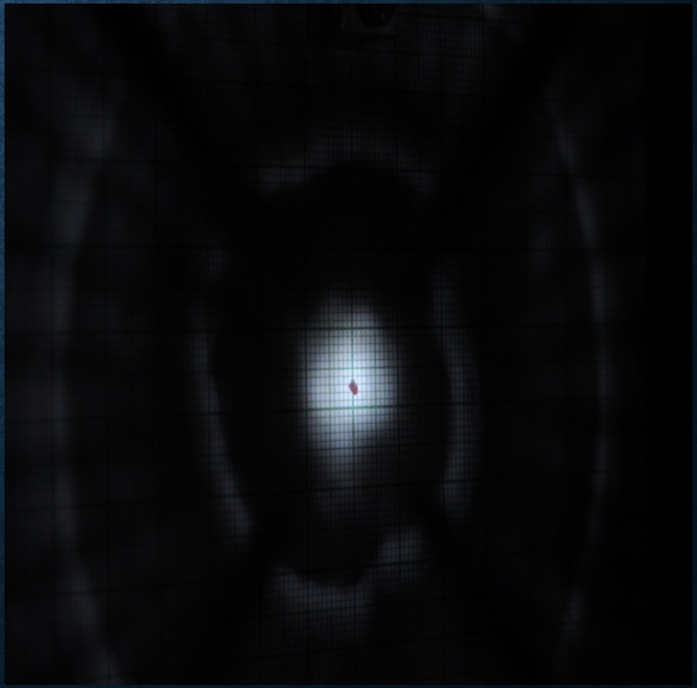

Angular Resolution (Half-power diameter) = ~3-4 arcmin
Field of View (1 CCD) = 41 x 41 arcmin

SXT- Focal Plane Camera Assy

Modified from Swift; Using spare MOS CCD22 from XMM: 600 x 600 pix, 40 microns

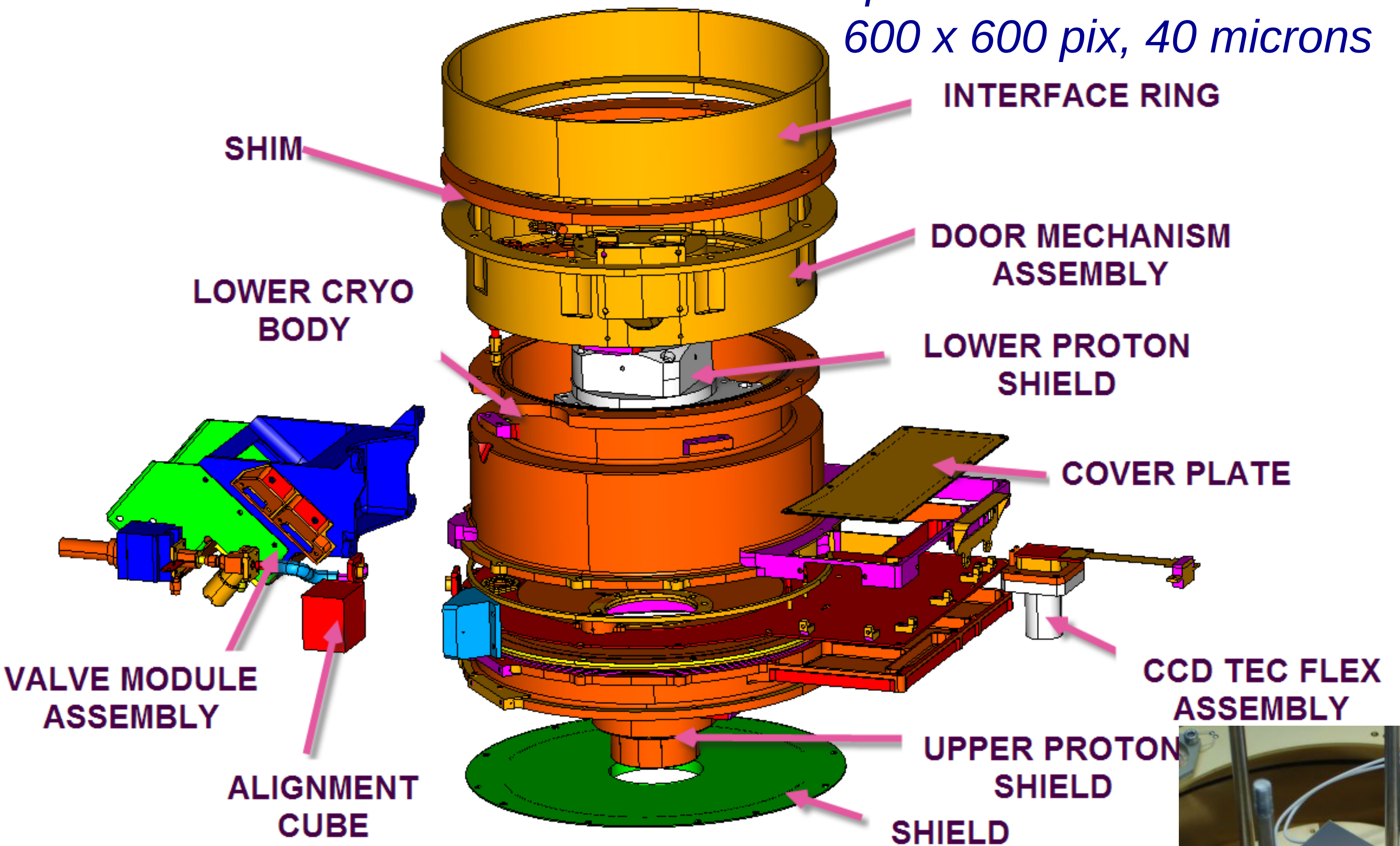

- Four Fe-55 calibration (corner) sources
- One Fe 55 calibration door source
- Thin Optical Blocking Filter
- CCD Assy. including TEC
- PCB with front-end electronics

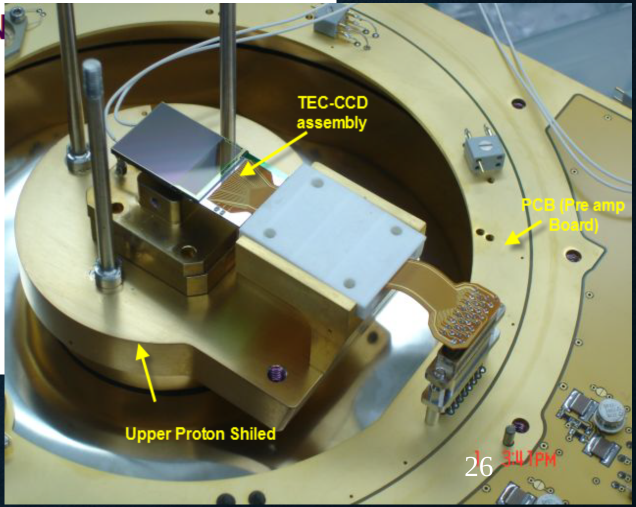

SXT CCD – Calibration sources and the filter image

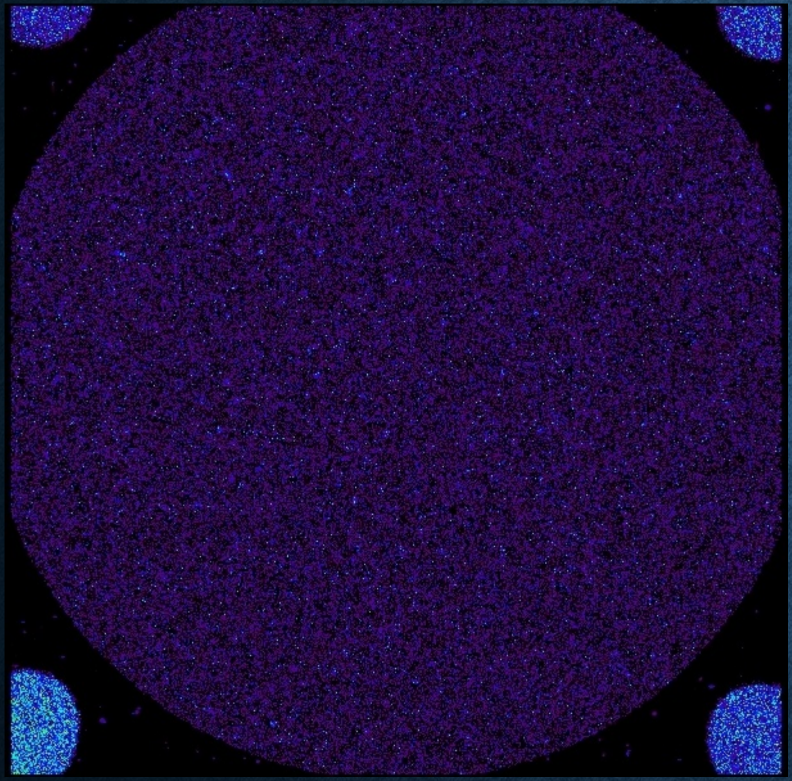

Door and Corner X-ray Calibration Sources
CCD: 600x600 pixels; 40 micron each

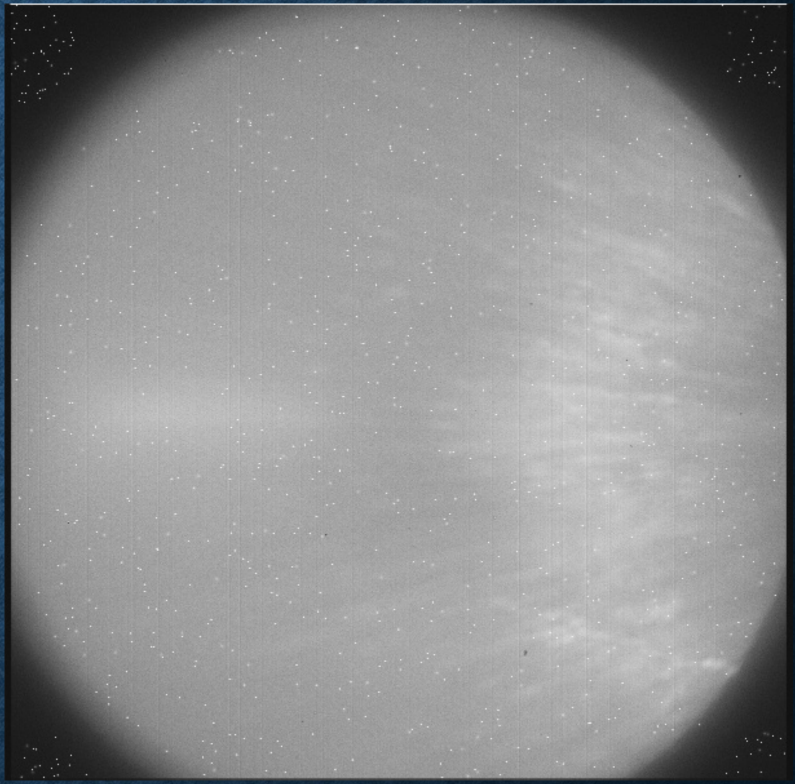

Optical LED Image of the filter

THIN FILTER TO ALLOW X-RAYS BUT BLOCK THE OPTICAL LIGHT

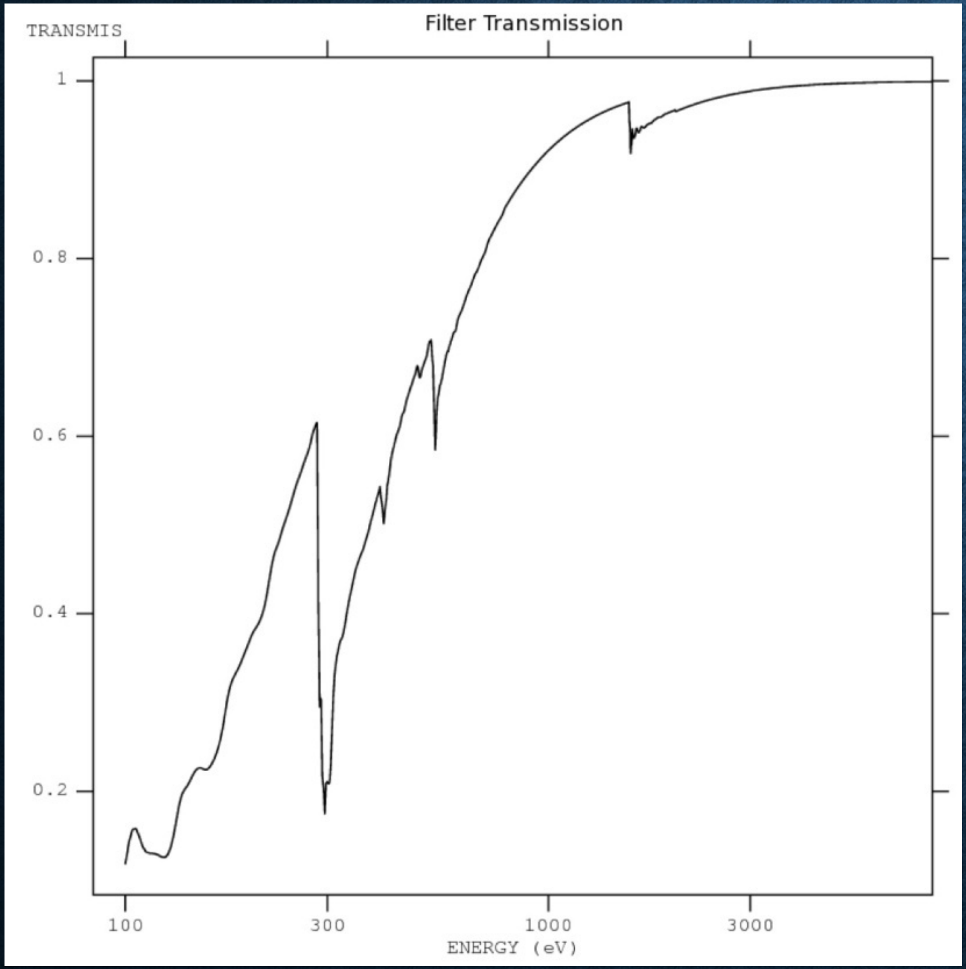

The filter design similar to the thin filter in XMM-Newton and Swift XRT.

It provides ~7 magnitude of optical extinction over the visible band.

For the Swift XRT with a PSF of ~15” a 6th magnitude star gives an optical loading of a few e- per pixel, at which point the quality of the X-ray data begins to be affected.

For the SXT with a ~7-8 times larger PSF and ~2 times larger angular size of the pixel the safe optical limit is expected to be closer to a ~4th magnitude star,

SXT : Area, Resolution, Sensitivity

- Effective area
  - ~75 cm^2 at 1.5keV
  - Sensitivity : $2x10^{-13}$ ergs cm^{-2} s^{-1} (5-sigma detection in about 25ks)
- Energy resolution
- 90eV@1.5keV, 136eV@5.9keV
- Moderate Time resolution
  - PC mode : ~2.4 s
  - FW mode : ~0.278 s
- Soft X-ray spectroscopy for sources with **2-10 keV flux > $3x10^{-12}$ ergs cm^{-2} s^{-1}**

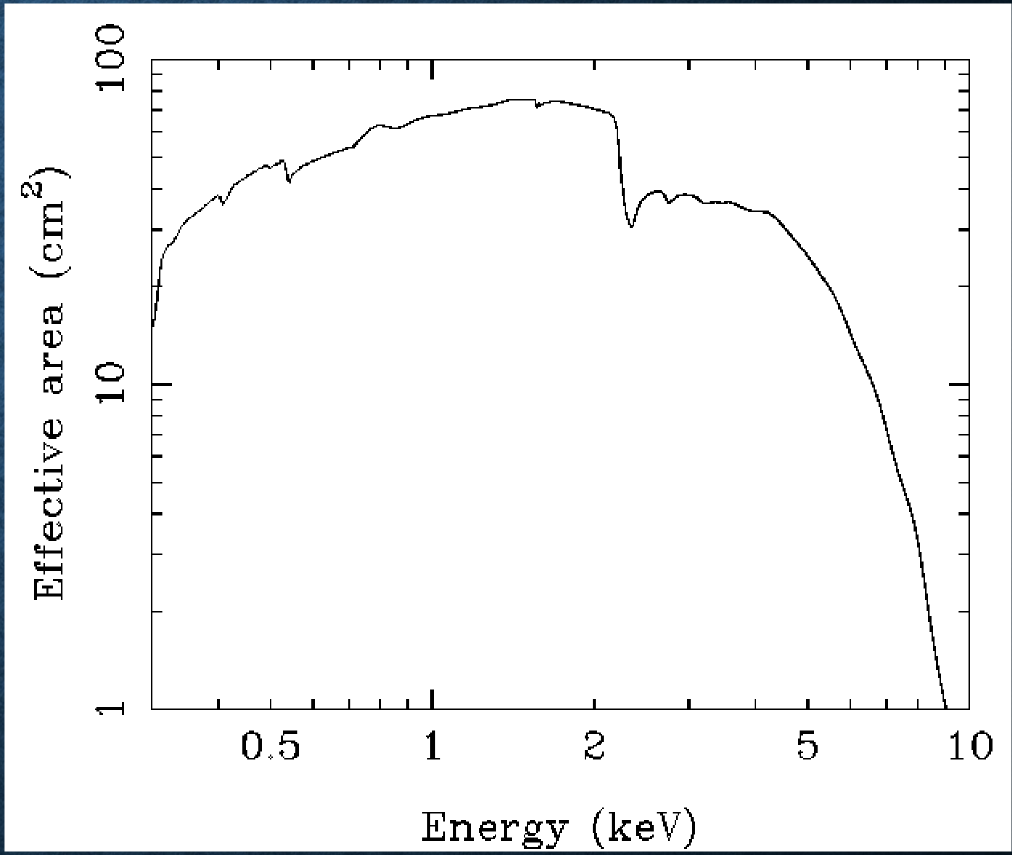

SXT SWITCH ON AND FIRST LIGHT

- Telescope (Optics) Door opening - 2015 Oct 15th
- Camera Door Opening - 2015 Oct 26th @ 06:30 UT
- First Light – 2015 Oct 26th (1976 Oct 27 – was my first rocket flight from Thumba)

Pointed at and observed- PKS2155-304 (Quasar) at redshift of 0.116 (1.6 Billion Ly away)

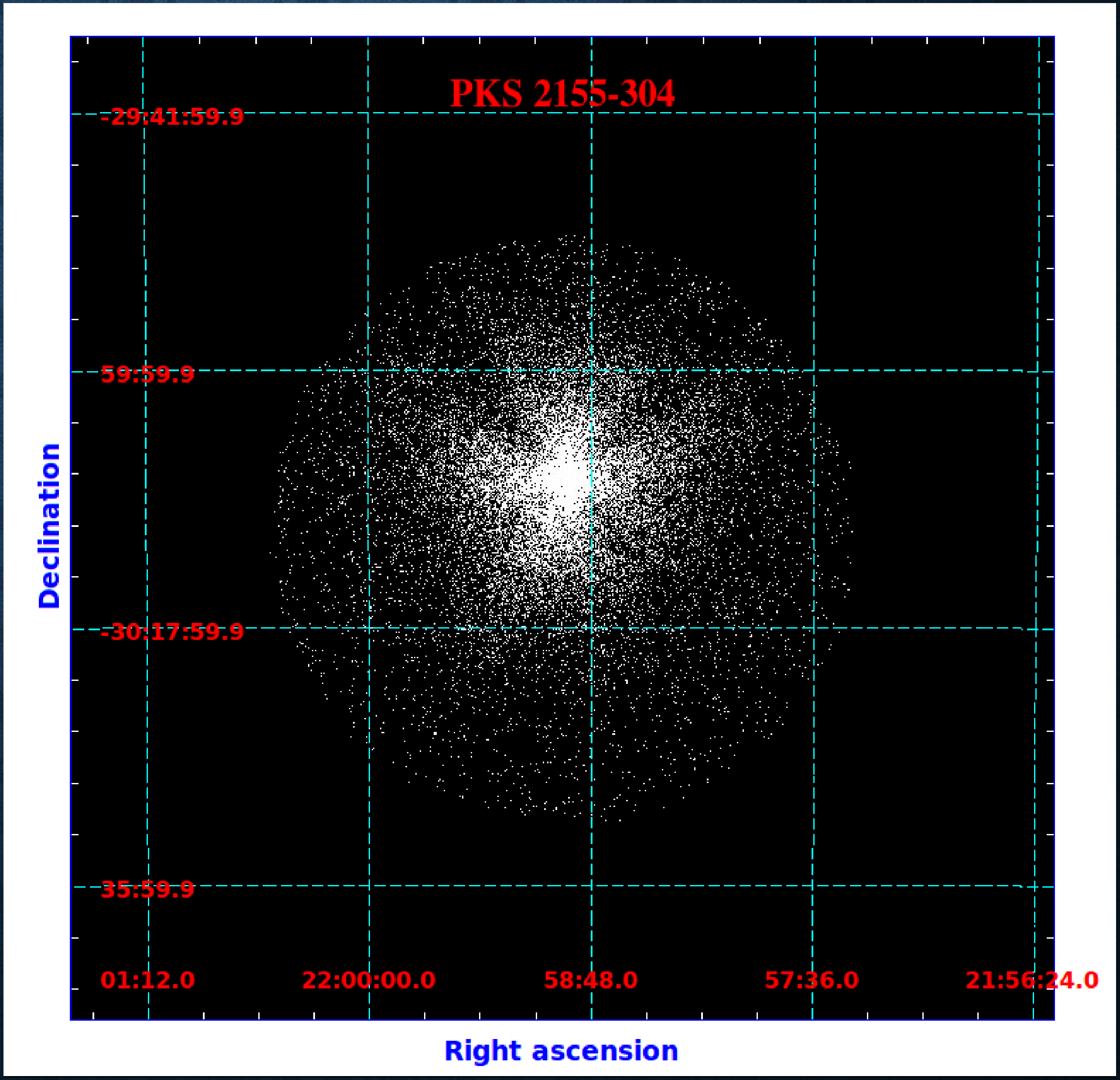

ANALYZING SXT DATA: READOUT MODES OF THE CCD (KOTHARE ET AL 2009)

1)Photon Counting Mode (PC), [Full foV: The Default Mode - includes the calibration sources]

2)Photon Counting Window Mode (PCW) – 5 pre-defined windows recommended.

3)Fast/Timing Mode (FM): reads only the central 150 x 150 pixels (10x 10 arcmin) of the CCD. For observing very strong cosmic sources like Crab, Cyg X-1 etc.

4)Bias Map Mode (BM), and

5)Calibration Mode (CM): where four small windows (each of size=80 x 80 pixels) covering only the corners are used for the corner radioactive sources in the CM. (A central 100x100 window is also used in the CM).

- X-ray spectral information available in all the modes.
- Time resolution in the PC, PCW, CM modes is 2.3775 s, and 0.278 s in the FM mode.
- Energy threshold applied only in PC, FW, PCW modes.

EVENT GRADES SELECTION

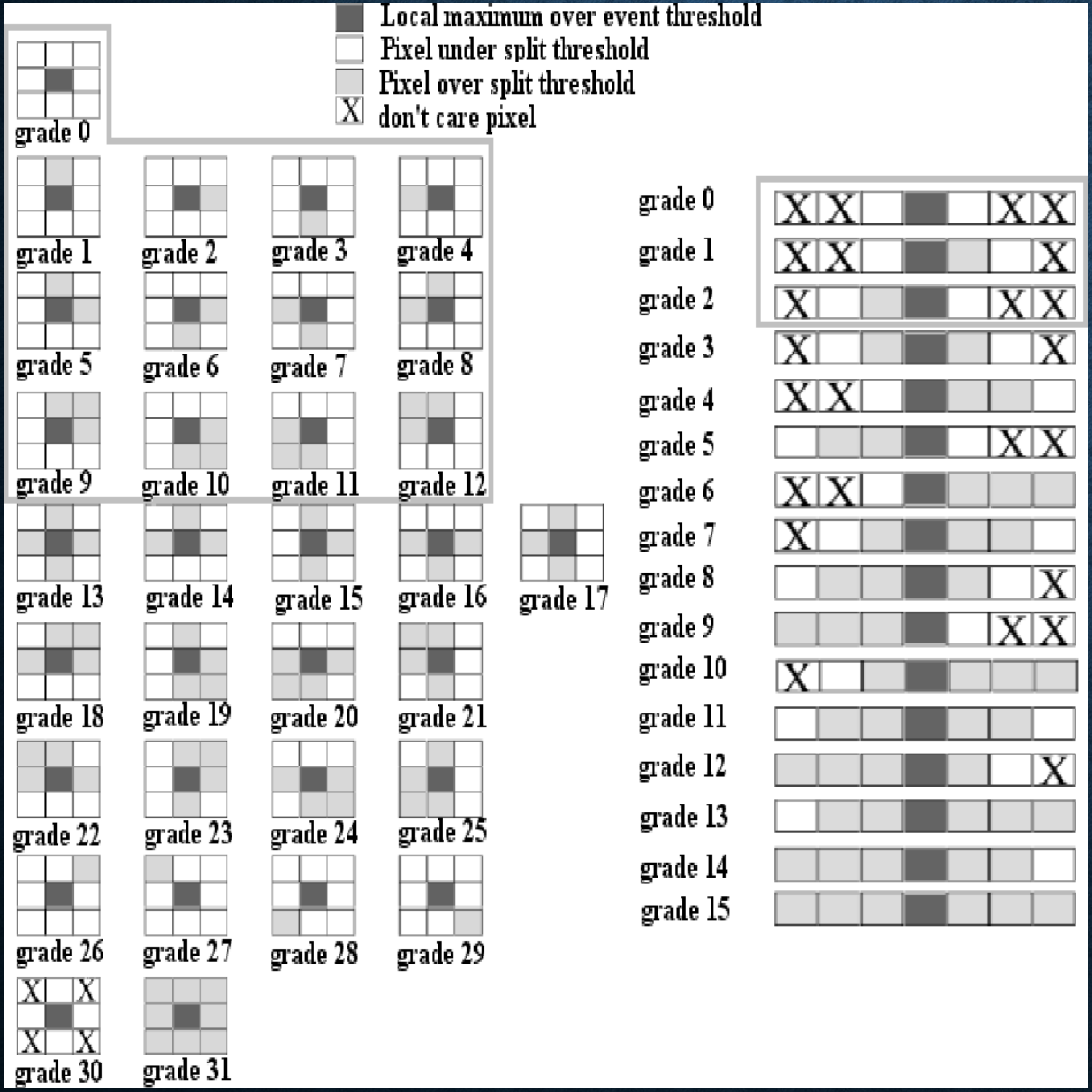

Default : 0-12

Response matrices available for

a) 0 grade
b) 0-4 grades
c) 0-12 grades

SXT: Analyzing Data

Level 1 SXT data from *each orbit* are run through the SXT pipeline at the SXT POC, and filtered for Bright Earth Avoidance, SAA, and events grades 0 to 12 only are accepted → Level2 orbit wise data – cleaned events, image. Light curve and spectra from the entire CCD frame.

A Julia/python tool is provided to merge Level2 data and remove all overlap of “gti’s” etc. create a single merged “events” file.

The merged events file can be read by “XSELECT” and final images, light curves and spectra can be created by the user.

The telescope area efficiency, detector response function and a deep background spectral and events file are provided to the user for further analysis

All products created using XSELECT are compatible with the HEASOFT pakage.

PKS 2155-304: BORE SIGHT, CALIBRATION

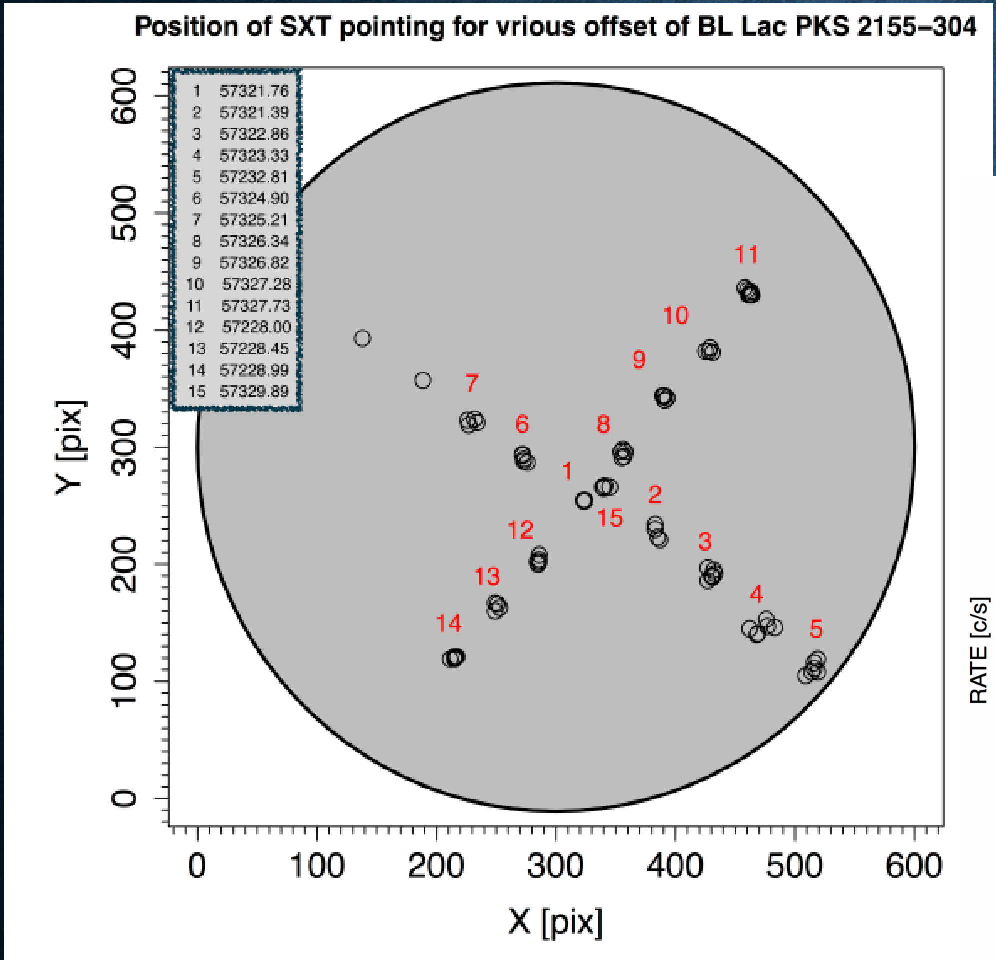

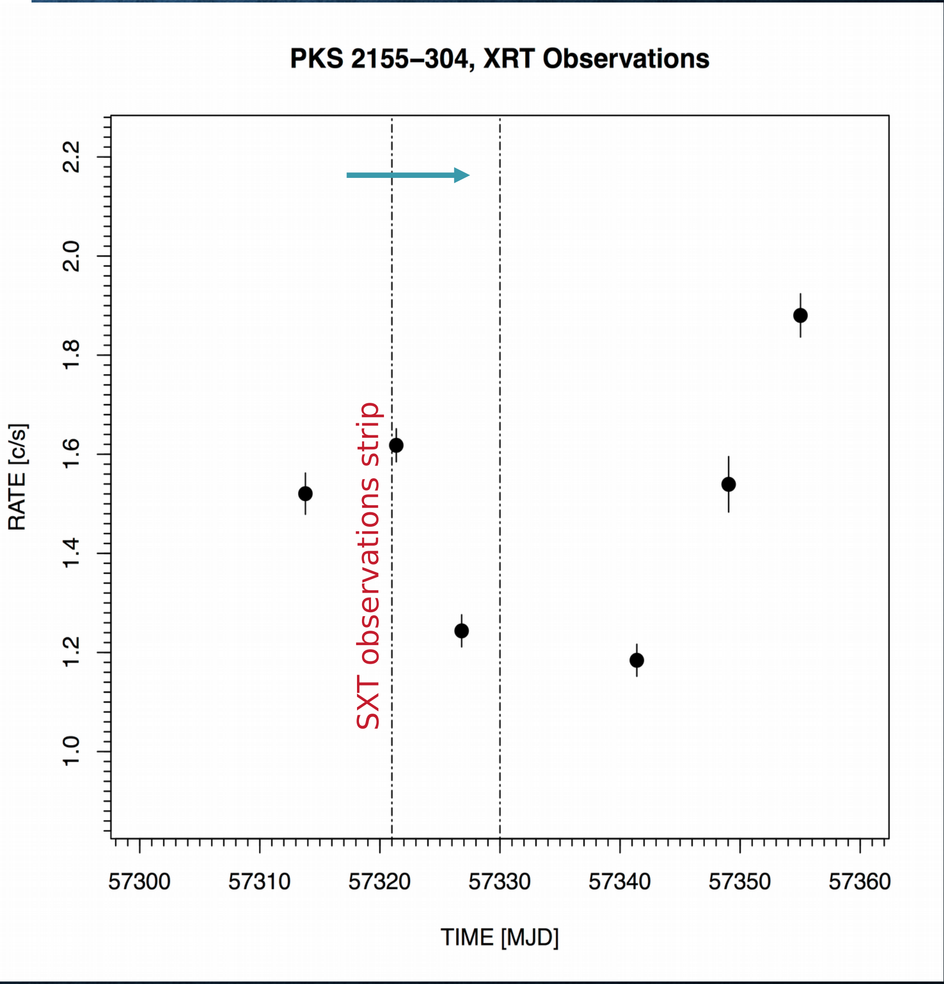

K.P.Singh

SXT Performance : Imaging

- PSF : 2' (FWHM), 10' HPD

Advantage : No pile-up for bright sources < 200 mCrab

Disadvantage: NO area in the detector for simultaneous background measurement

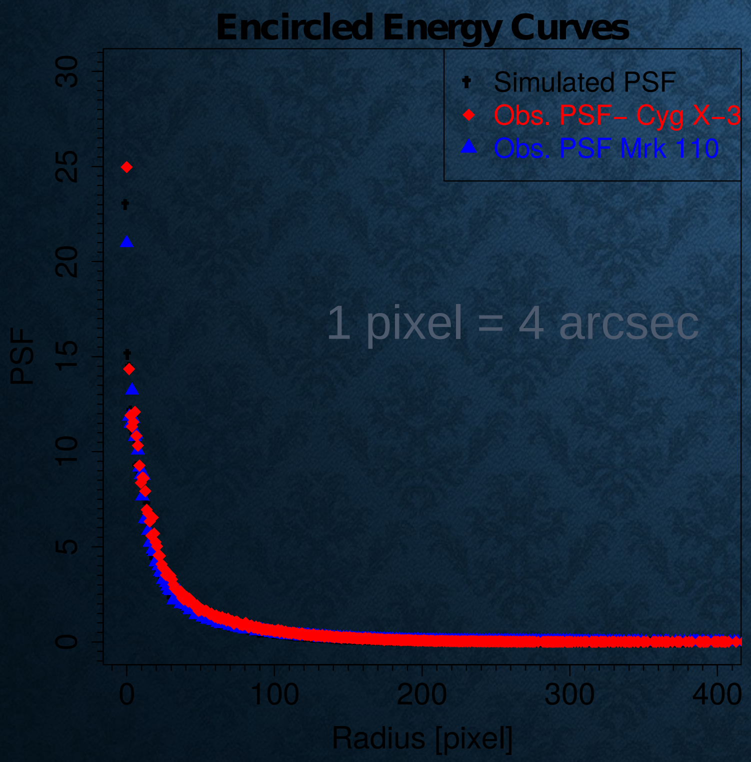

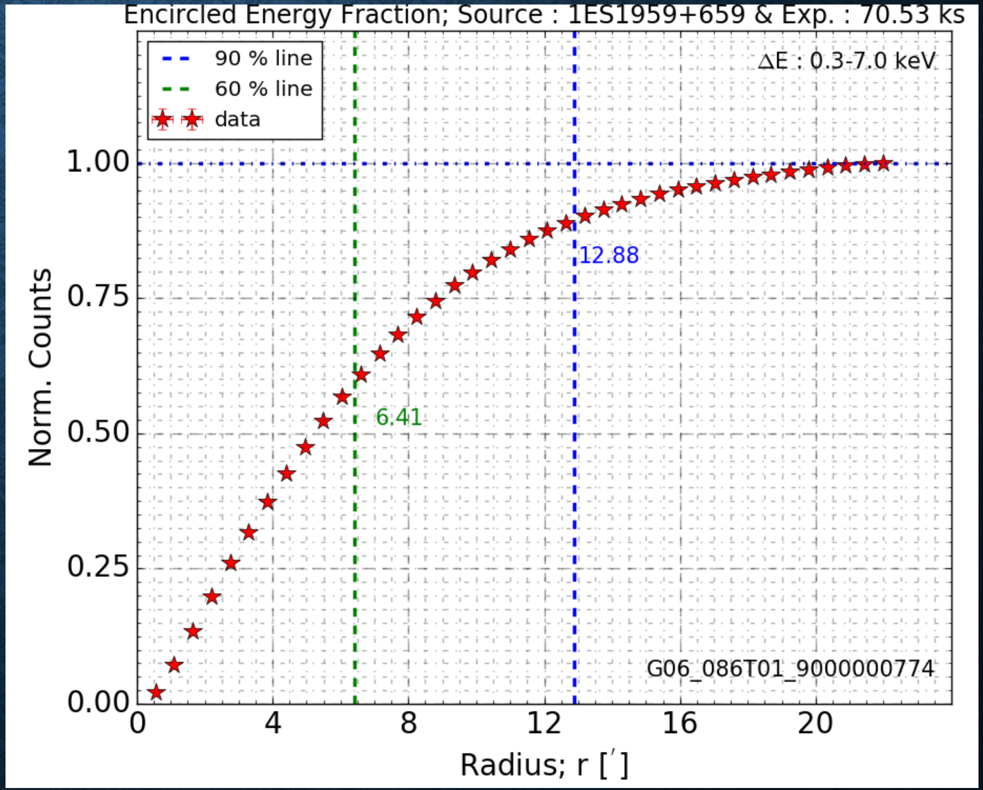

No significant energy or offset dependence

Vignetting function Using SNR 2E0102-7217

$$V(\theta) = 1 - C\theta^2$$

θ is the off-axis angle, and the coefficient C is a function of energy (in keV),

$$C(E) = P_0 \times \mathrm{P1}_{E} + P_2$$

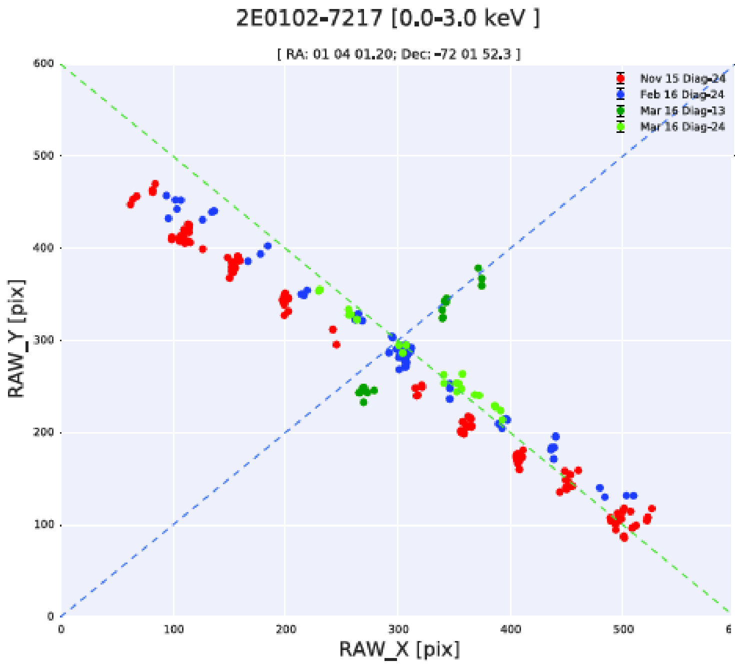

P_0 = -2.492e-06
P_1 = 0.9996
P_2 = 9.6120e-06

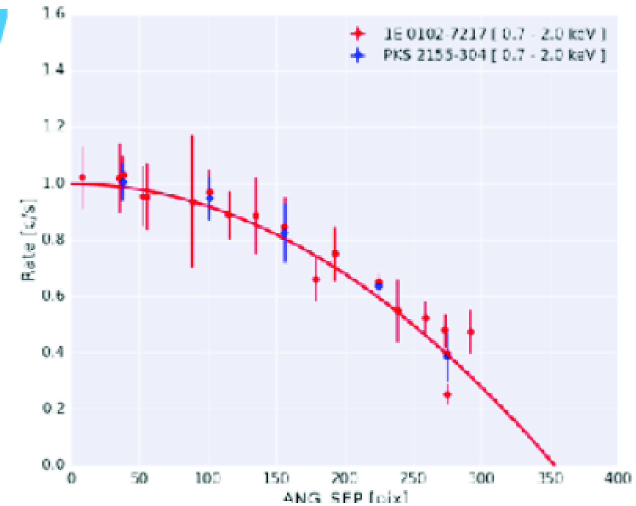

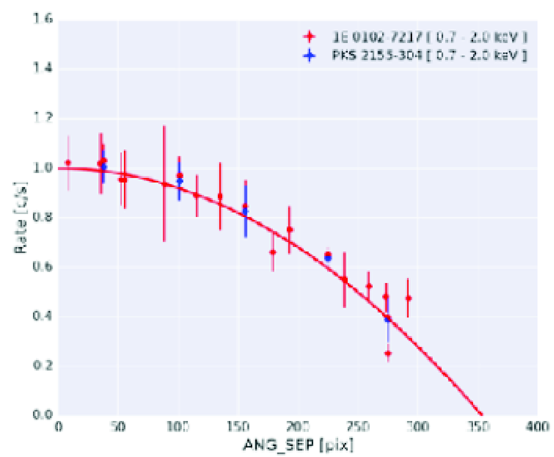

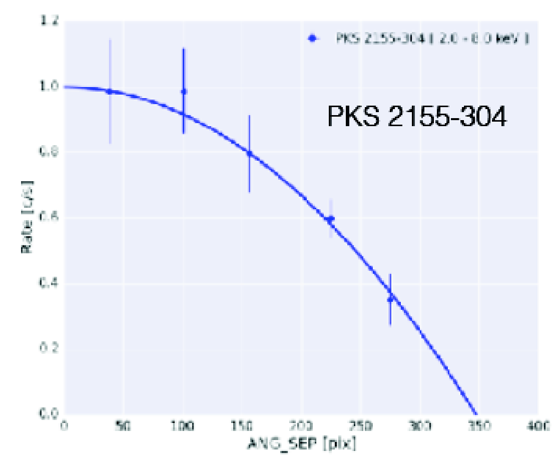

Singh et al. 2017, (Telescope Description and Calibration Status), In preparation

SXT Performance: Vignetting function

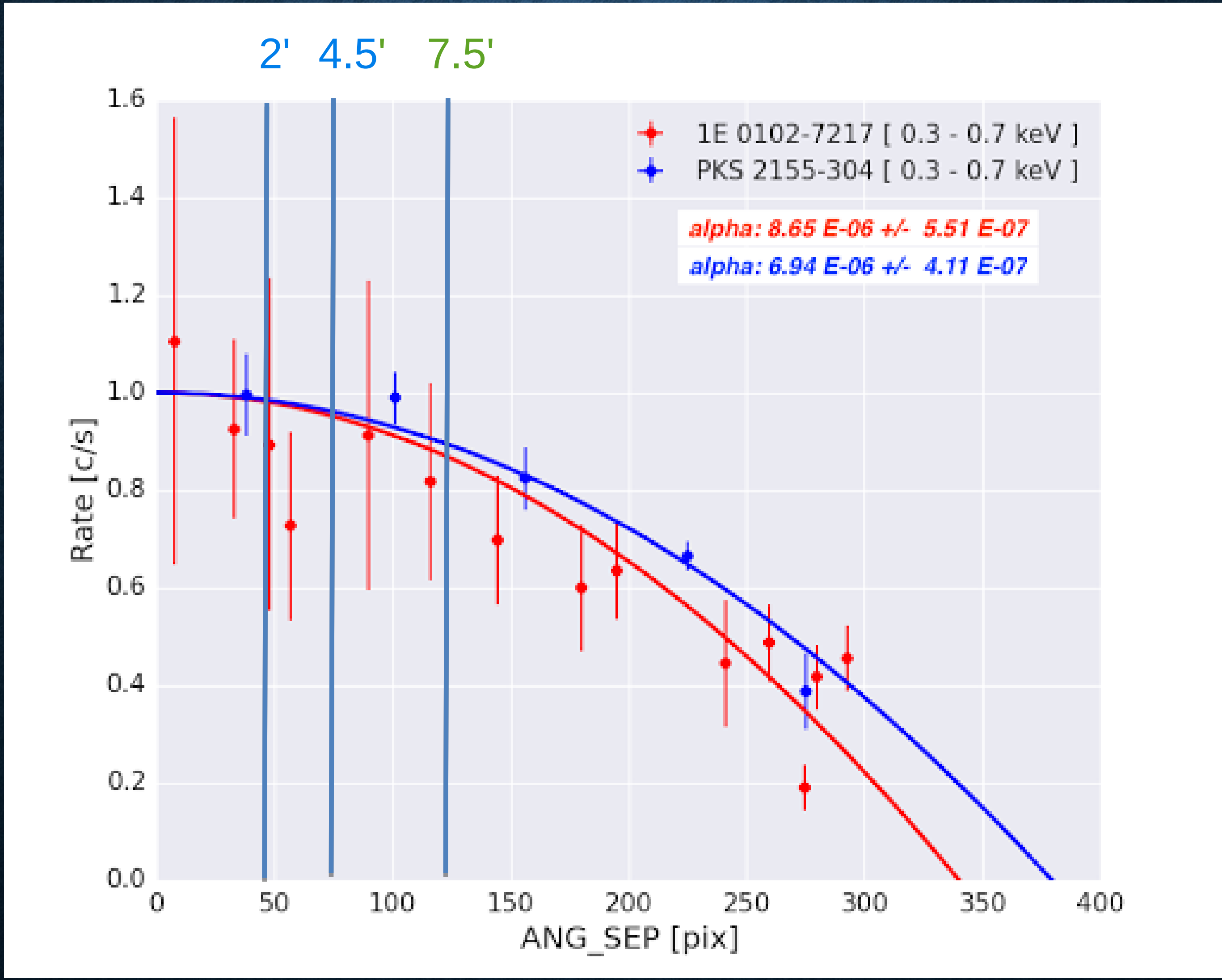

SXT Performance : Spectral Response

- ARF: recalibrated using Crab observations (Feb 2017), Issues at low energy < 0.5keV
- RMF : gain change ~ 20-40eV, issues at low energies, Above 0.5 keV okay with a few % systematic error (ARF/RMF need further corrections!)
- Background : Low and steady background, average background spectrum from blank sky observation available.

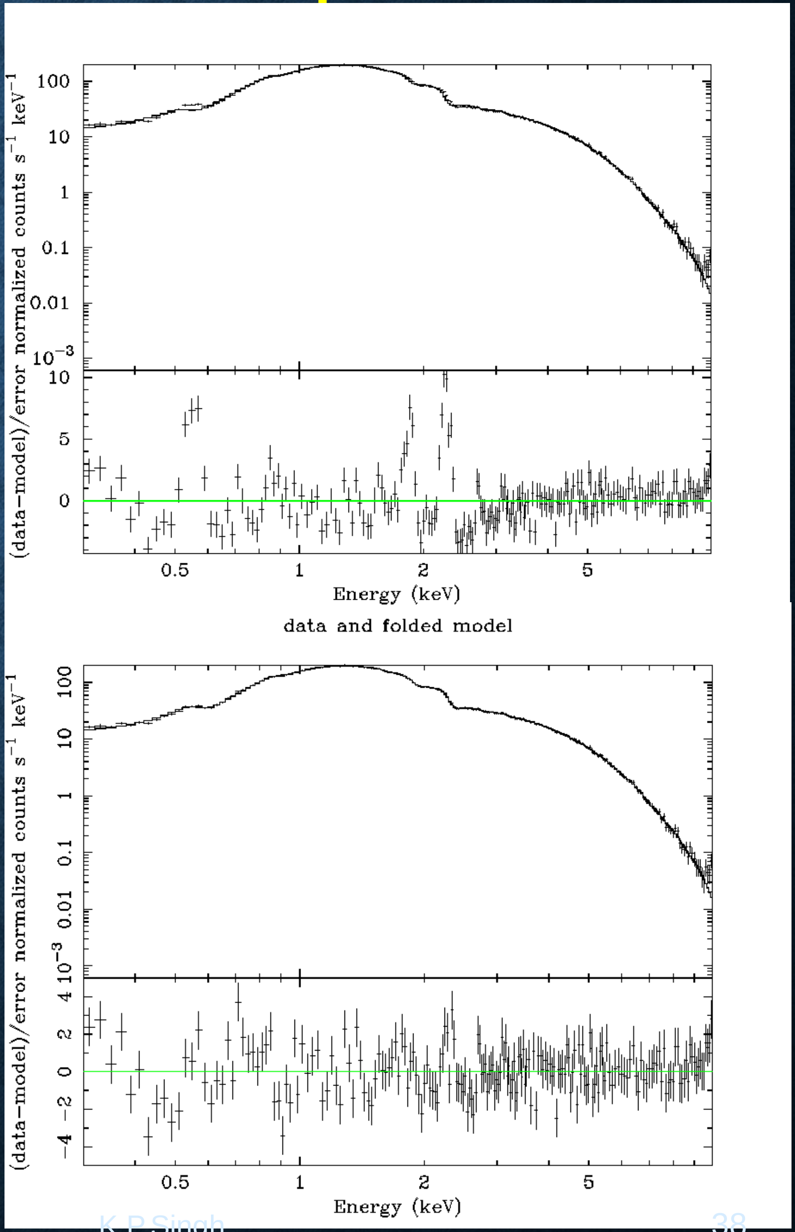

2E01020-72 – SNR in SMC: spectral response of the very soft band of the SXT

IACHEC Model: Plucinsky et al. 2016

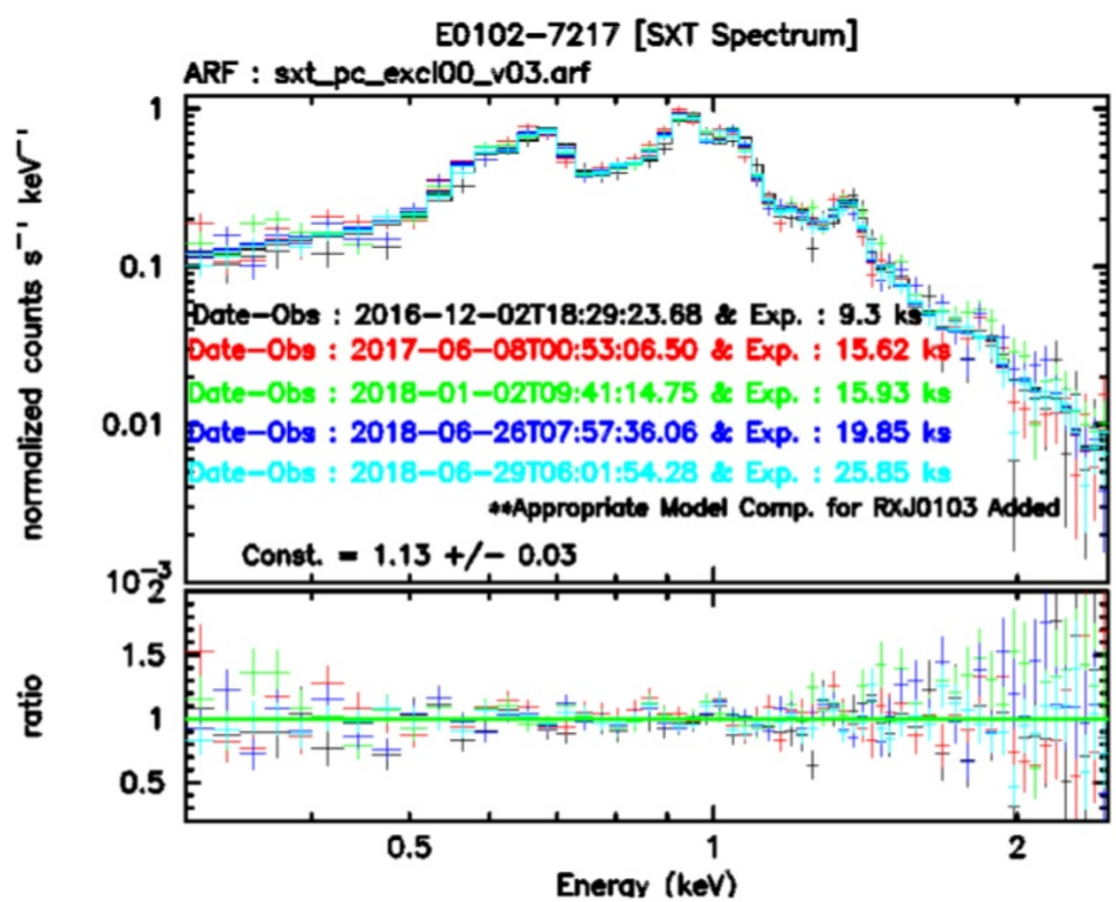

Figure 3.11: The X-ray spectrum of 1E0102-72.3 as fitted with the IACHEC model derived from several X-ray observatories carrying a CCD camera in the focal plane of a telescope. The SXT spectrum was extracted from a radius of 10 arcmin. A significant contributions from the closest (<2arcm) XRB are noticed and fitted with appropriate model component.

Credits:
S. Chandra
+ SXT team

SXT: Tycho Super Nova Remnant

1572 A.D.

~445 years old SNR

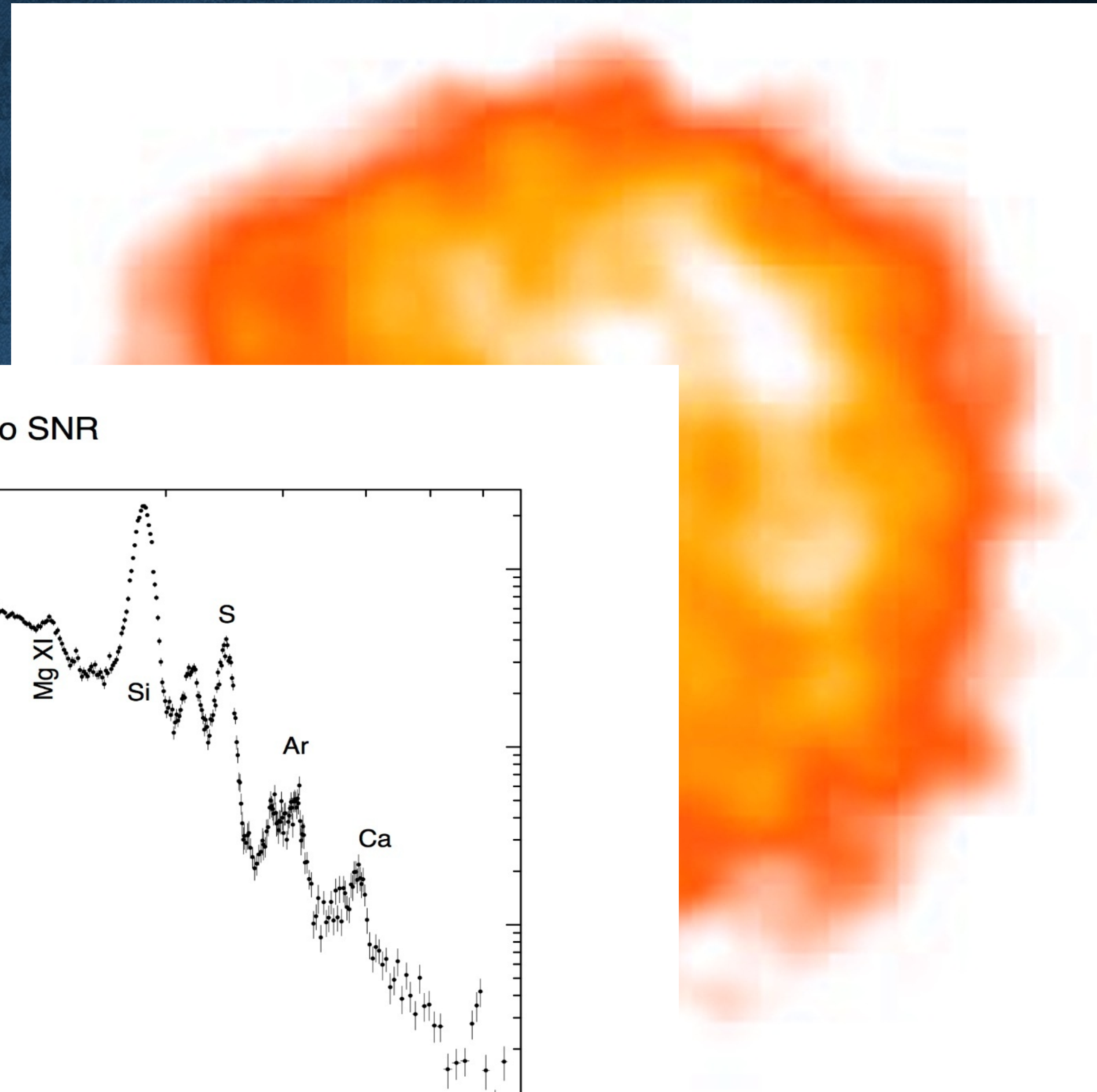

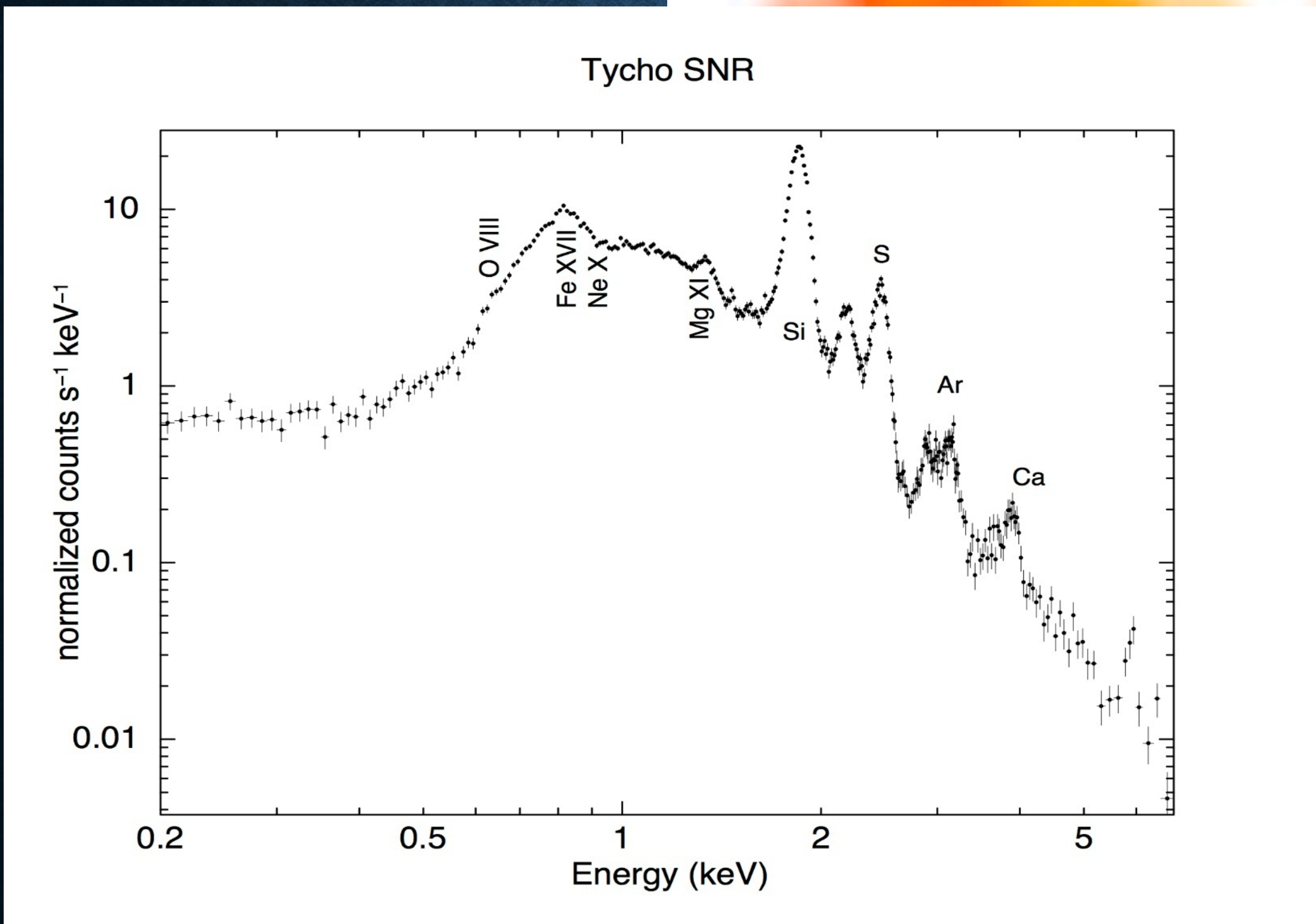

Tycho SNR

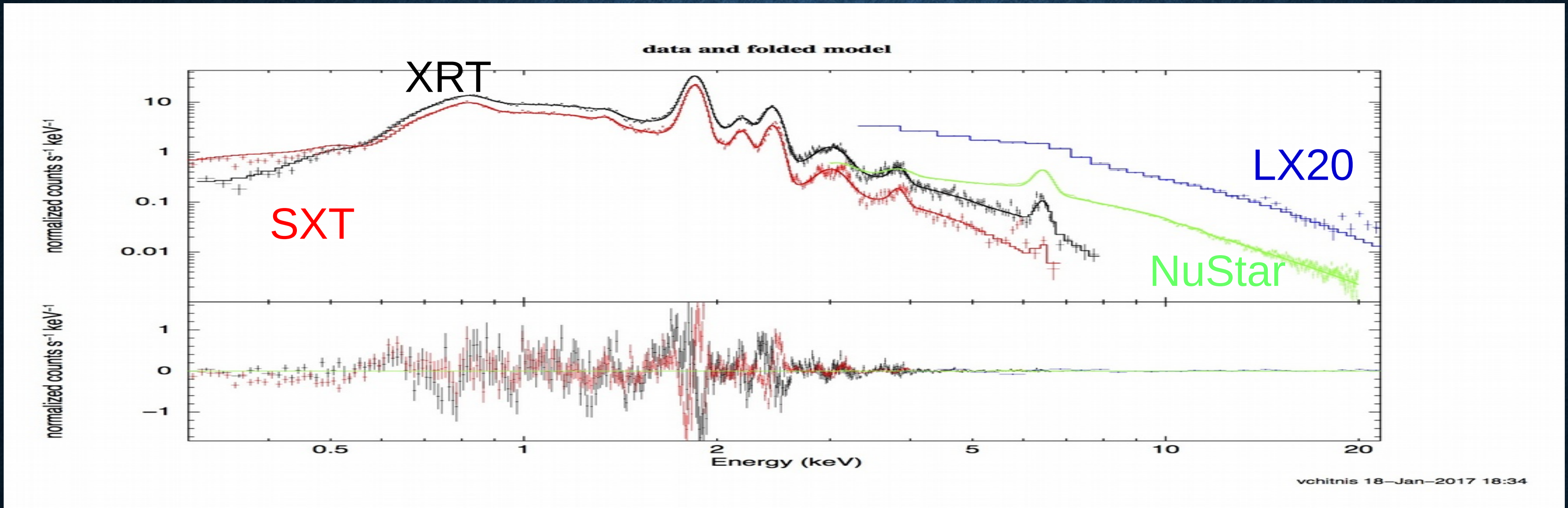
data and folded model
XRT
SXT
LX20
NuStar
normalized counts s^{-1} keV^{-1}
10
1
0.1
0.01
0
−1
0.5
2
5
20
Energy (keV)
vchitnis 18–Jan–2017 18:34

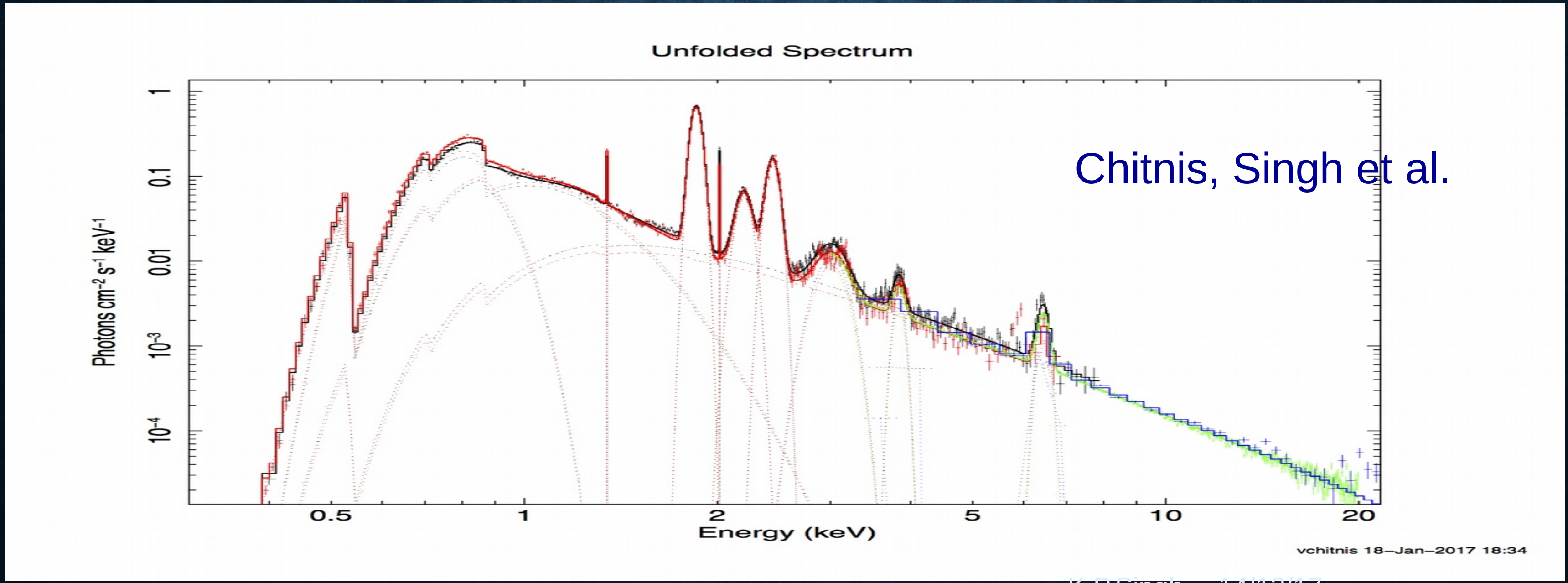
Unfolded Spectrum
Chitnis, Singh et al.
Photons cm^{-2} s^{-1} keV^{-1}
1
0.1
0.01
10^{-3}
10^{-4}
0.5
2
5
10
20
Energy (keV)
vchitnis 18–Jan–2017 18:34

CAS A: BREMSS + 2 PL + 10 GAUSSIANS (SXT, XRT, NUSTAR)

N_H=8 x 10^{21}cm^{-2}
kT=1.1 keV

Lines at
1.85 keV Si
2.44 keV S
0.94 Fe-II
1.35 Mg ?
3.13 Ar ?
3.91 Ca ?
2.0
2.19
6.62 Fe
7.73 keV

NEI reqd

Γ=2.44 (SXT+XRT)
Γ=3.28 (NuStar)

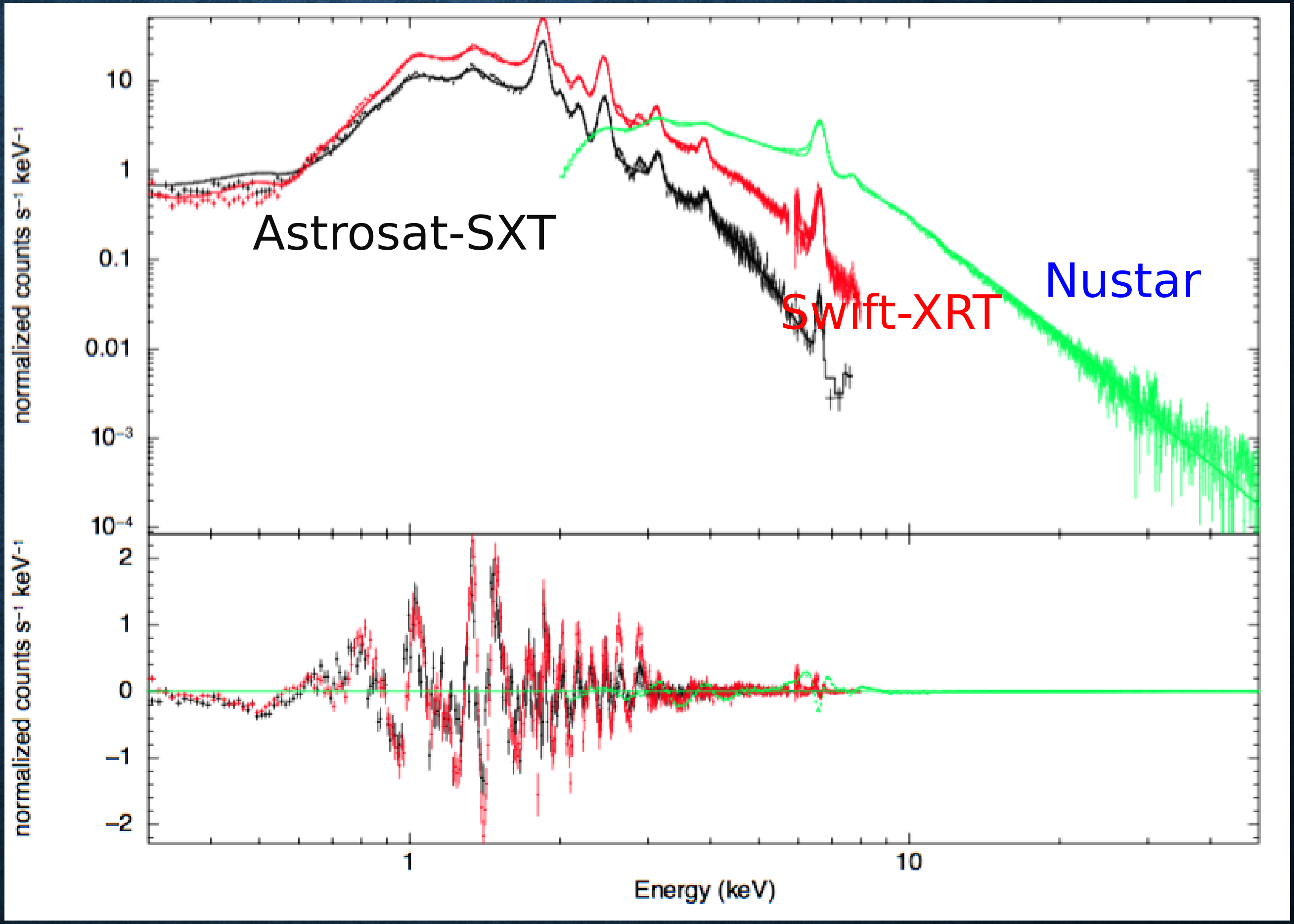

SWIFT XRT (in Red) and SXT (black) and NuStar (green) Spectrum comparison
Credits; V. Chitnis + SXT team (TIFR)

NGC 4151:
SXT AND LAXPC - A COMPARISON OF BACKGROUNDS

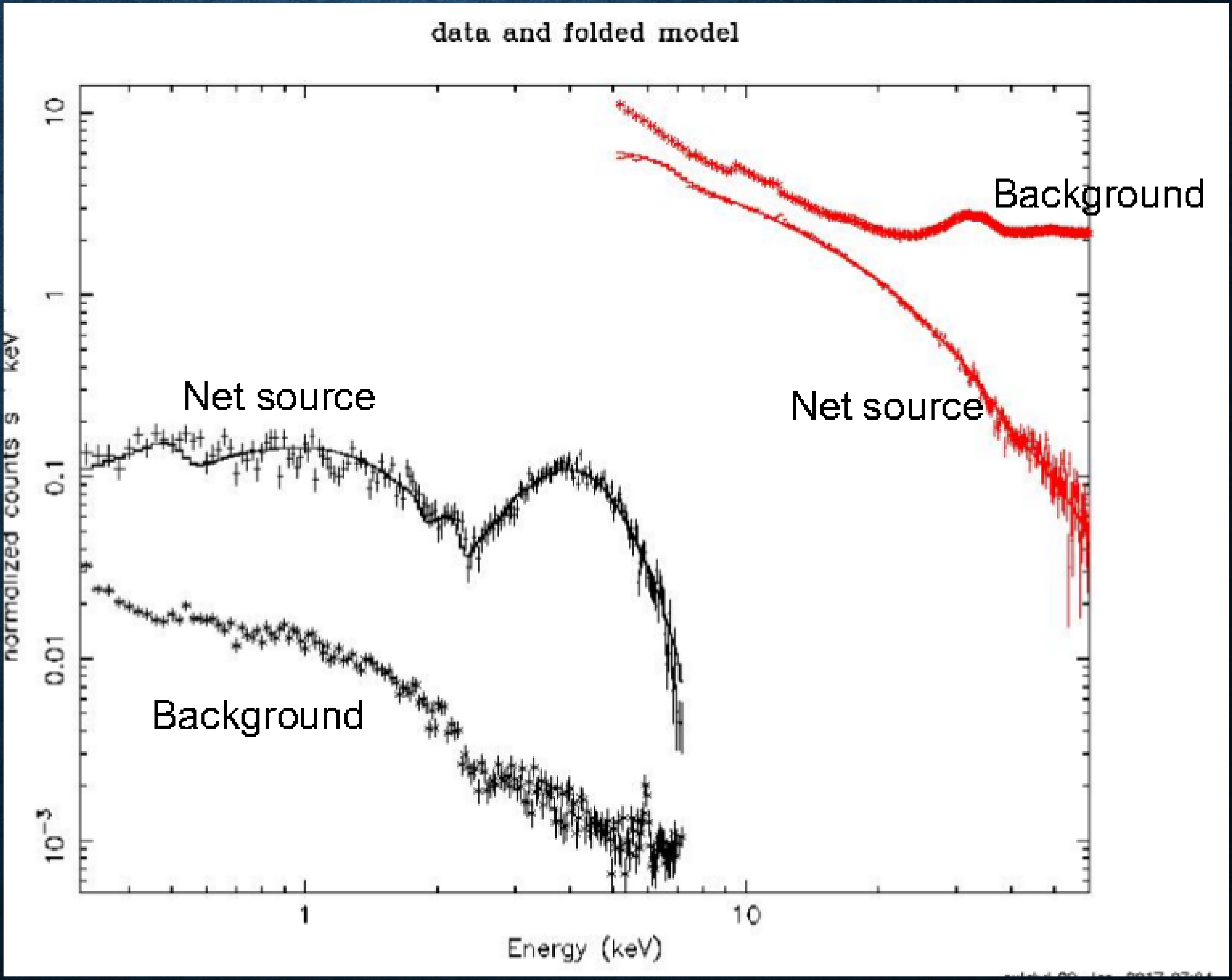

Mar 14-16, 2016: PV data

NGC 4151: SXT+LAXPC SPECTRUM OVER A WIDE X-RAY BAND

Absorbed PL (0.3-5keV, 7-10, 40-60keV)

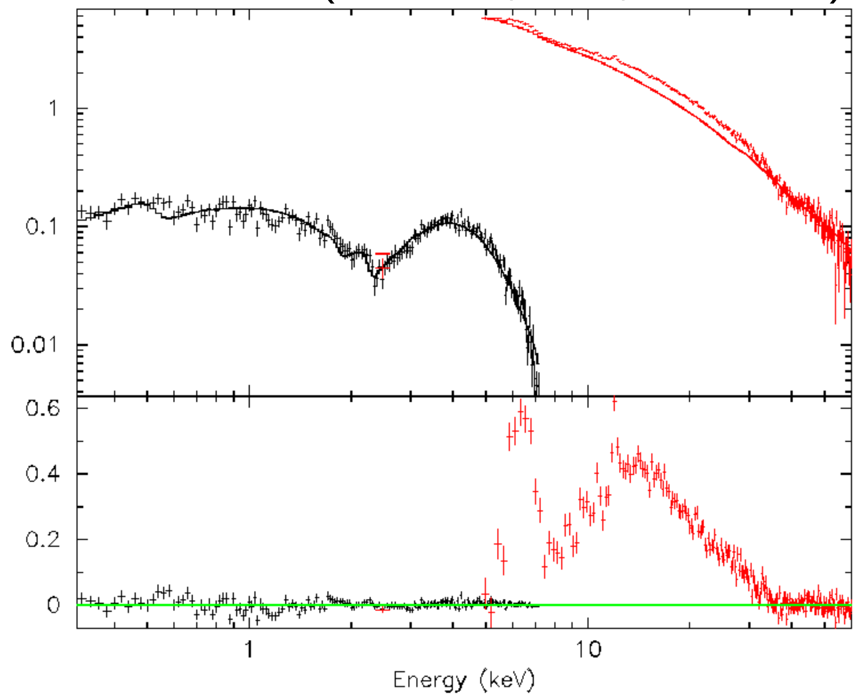

pcfabs*(pexrav + gauss)

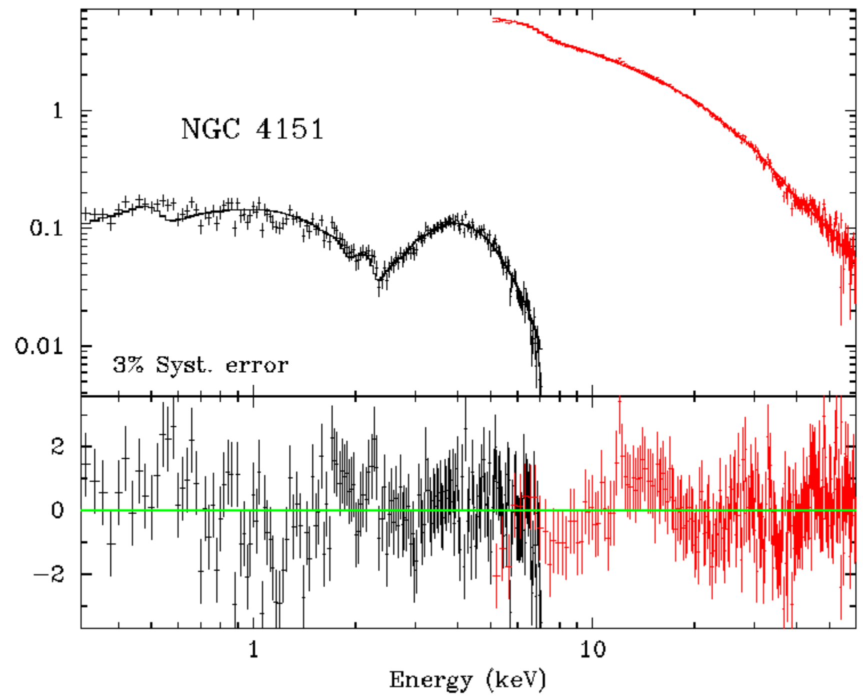

Reduced chi^2 = 1.3

V3890 SGR: A RECURRENT (28 YRS) - 1962, 1990 SYMBIOTIC NOVA: 6 KPC AWAY, P=519.7D, SN IA PROGENITORS(2019/08/27) DAYS 8-10

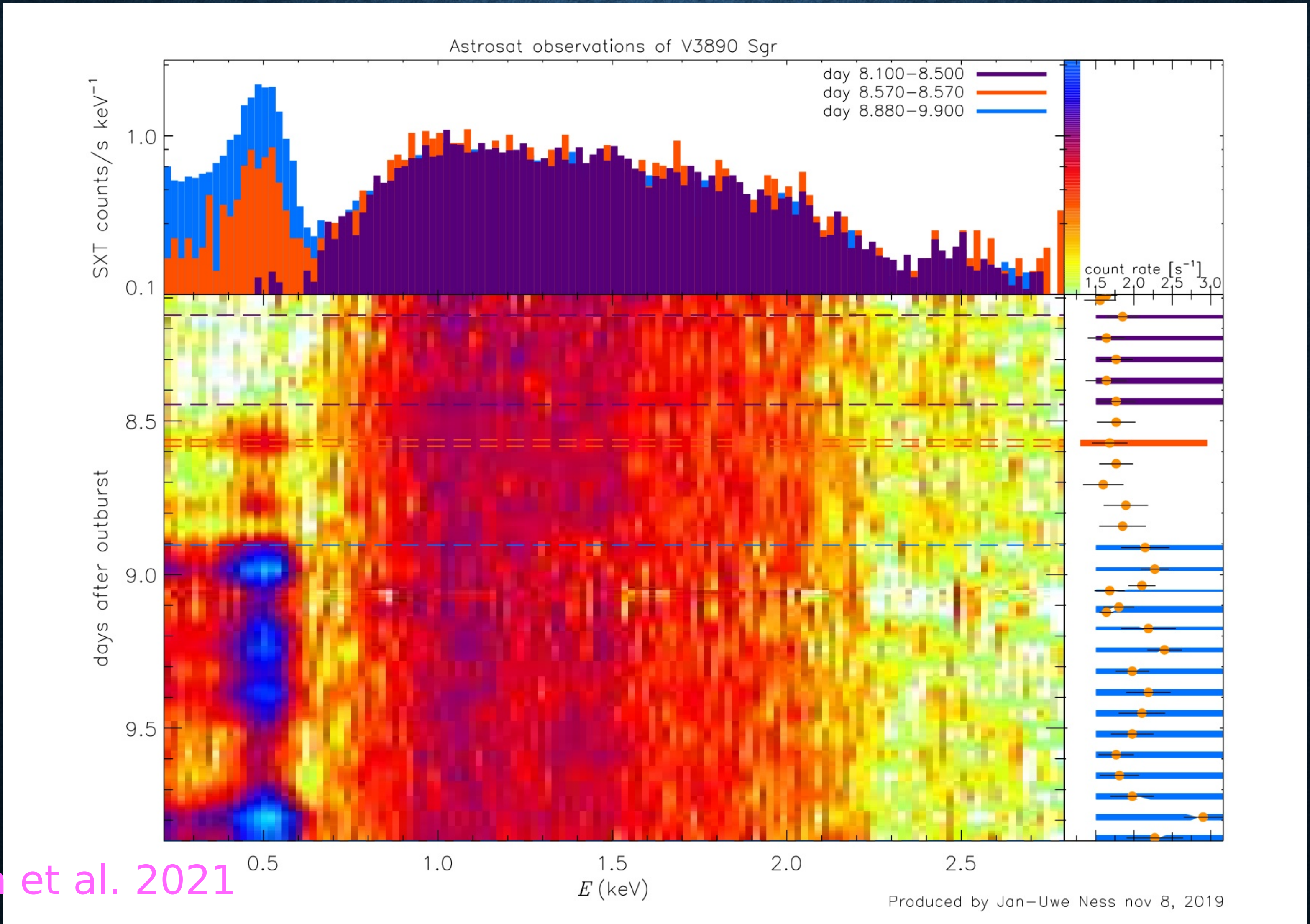

Singh et al. 2021

V3890 SGR : DAYS 15-19 WITH SXT

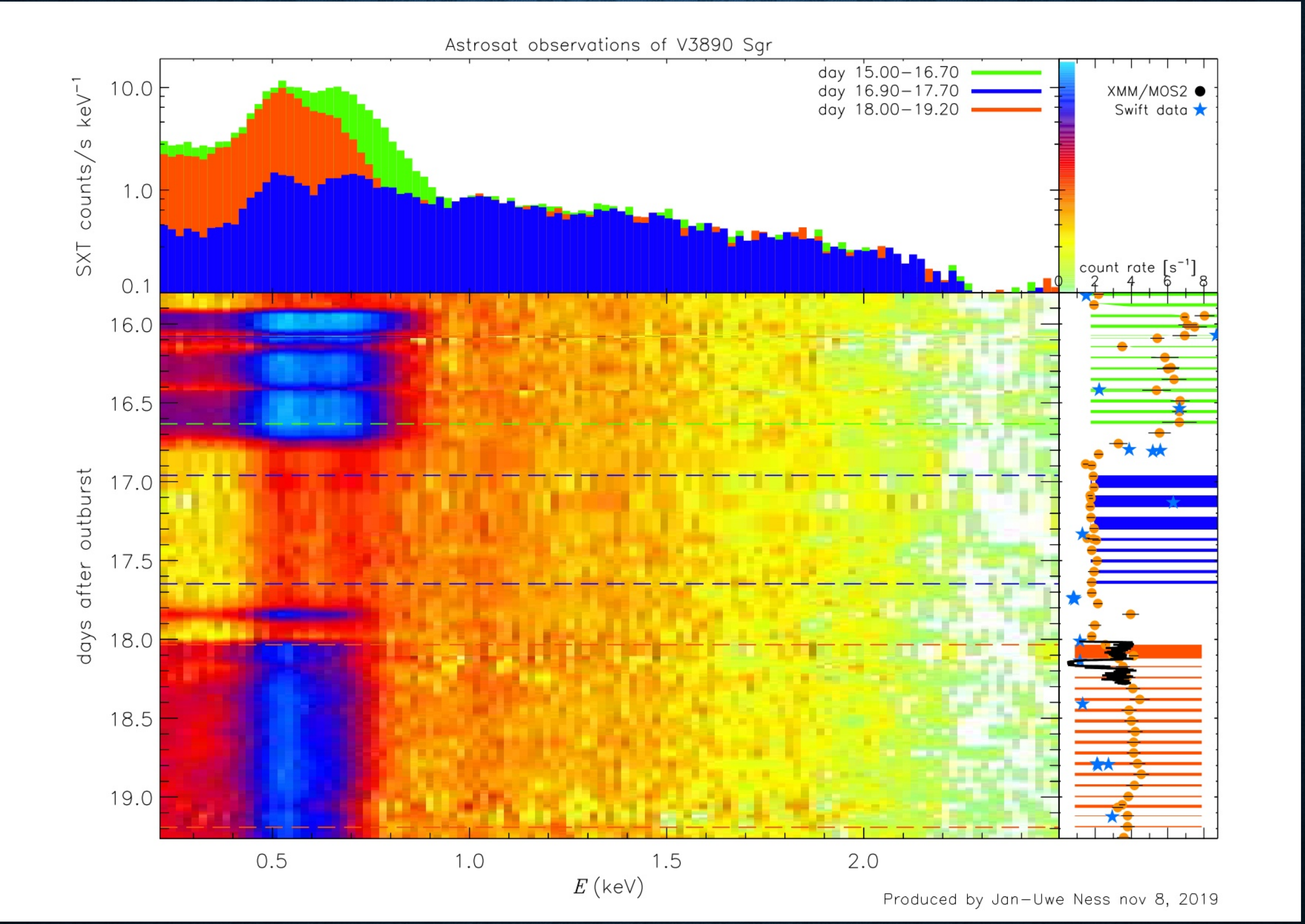

M31N 2008-12a: SXT 2020-11-10/12

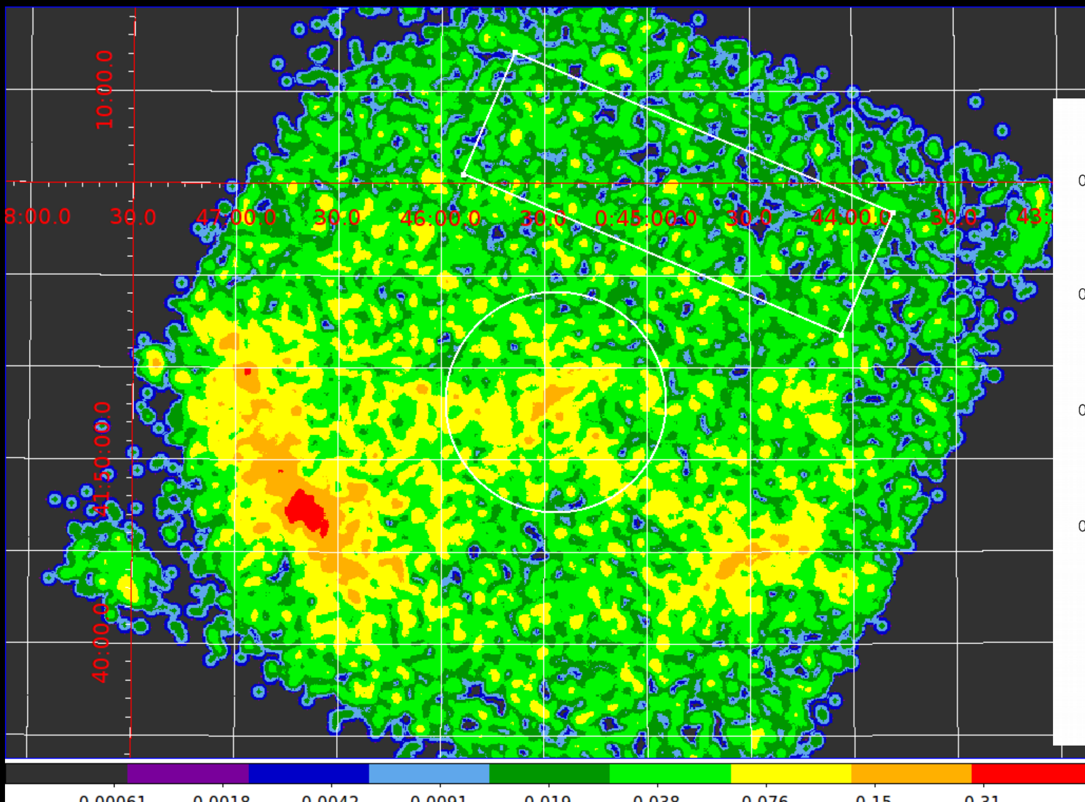

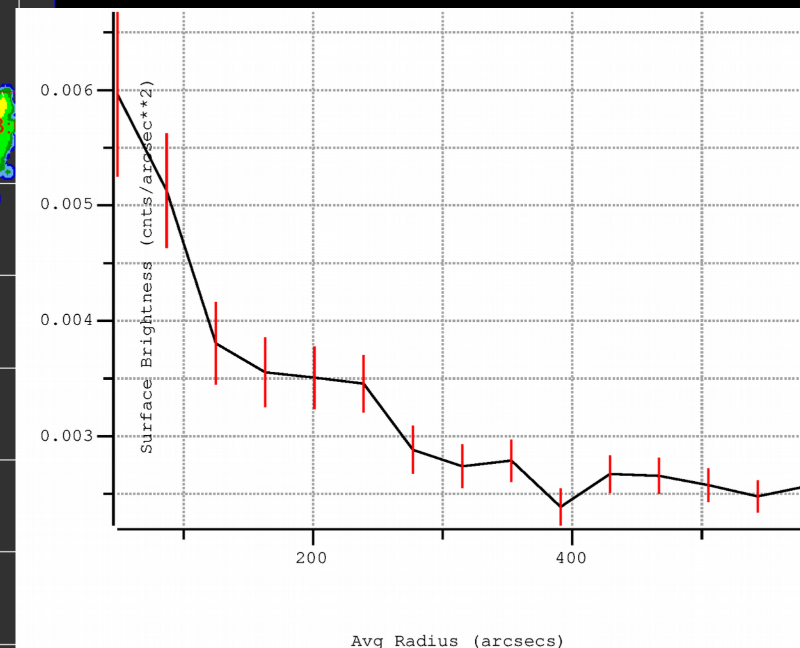

AstroSat SXT 2020 Nov 10-12. Exposure time = 57530s;
0.01100 +- 0.00075 counts per sec (14 σ detection)

M31N 2008-12a: SXT spectrum

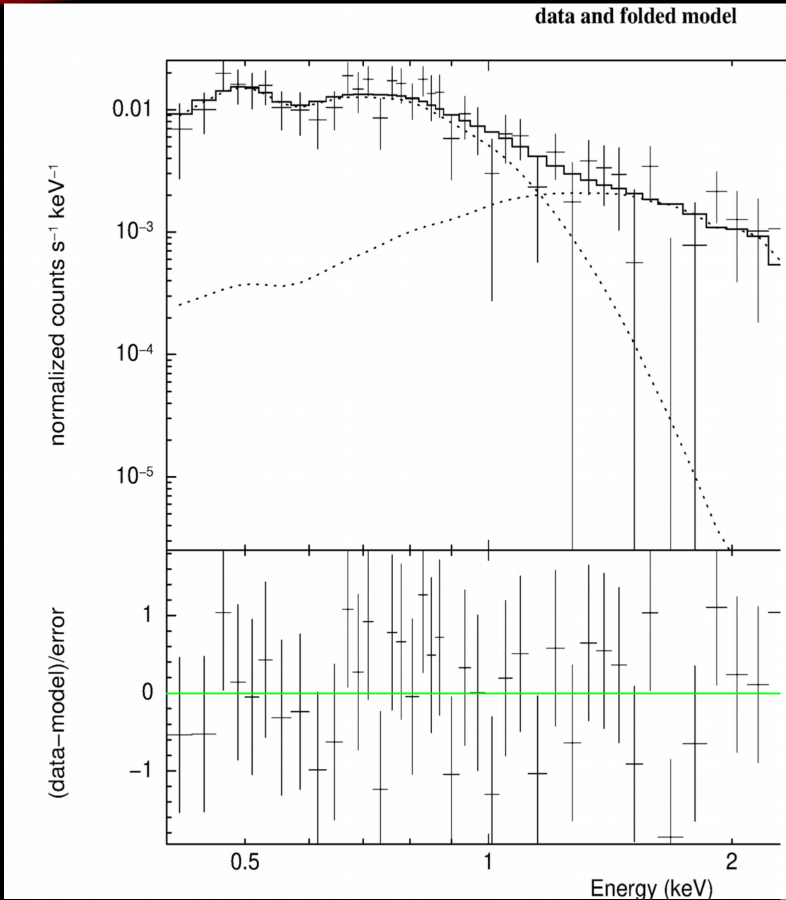

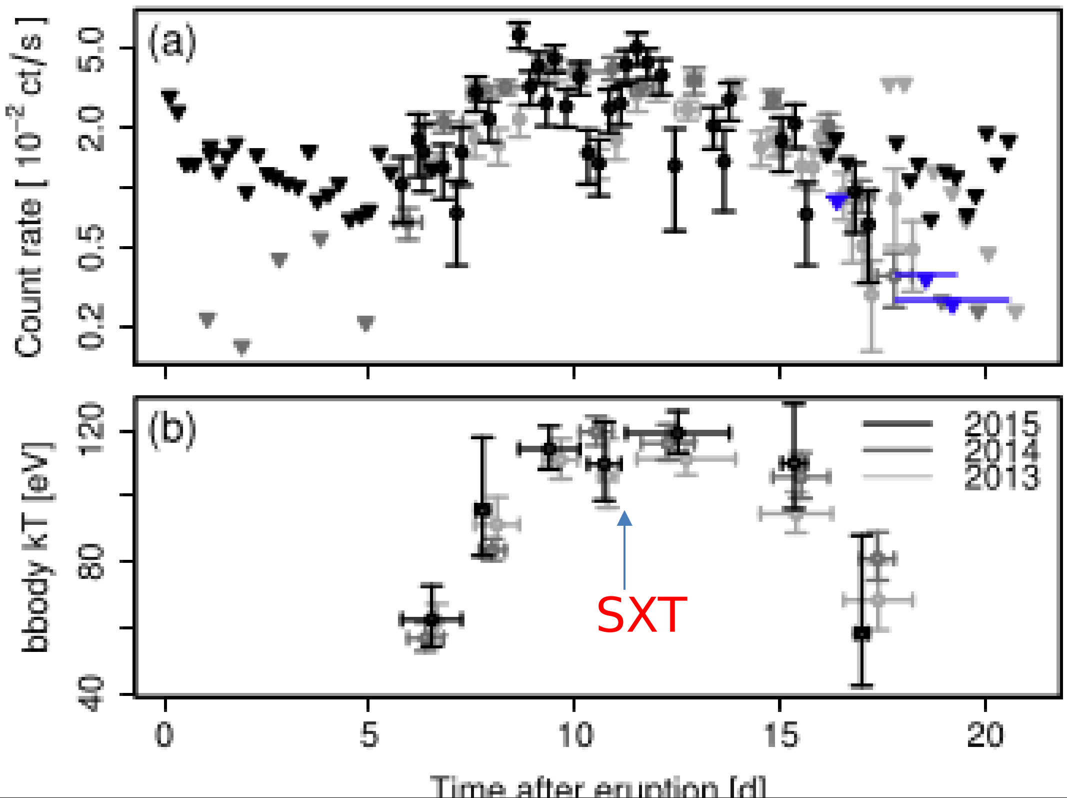

kT(bbody)=95 eV +- 10 eV; Plasma solar apec kT >4 keV

Flux (0.3-10 keV)=8.8 x 10^{-13} ergs/cm2/s

Lx = 6.3 x 10^{37} ergs/s

PROXIMA CEN (M-DWARF)

31/5 – 1/6, 2017

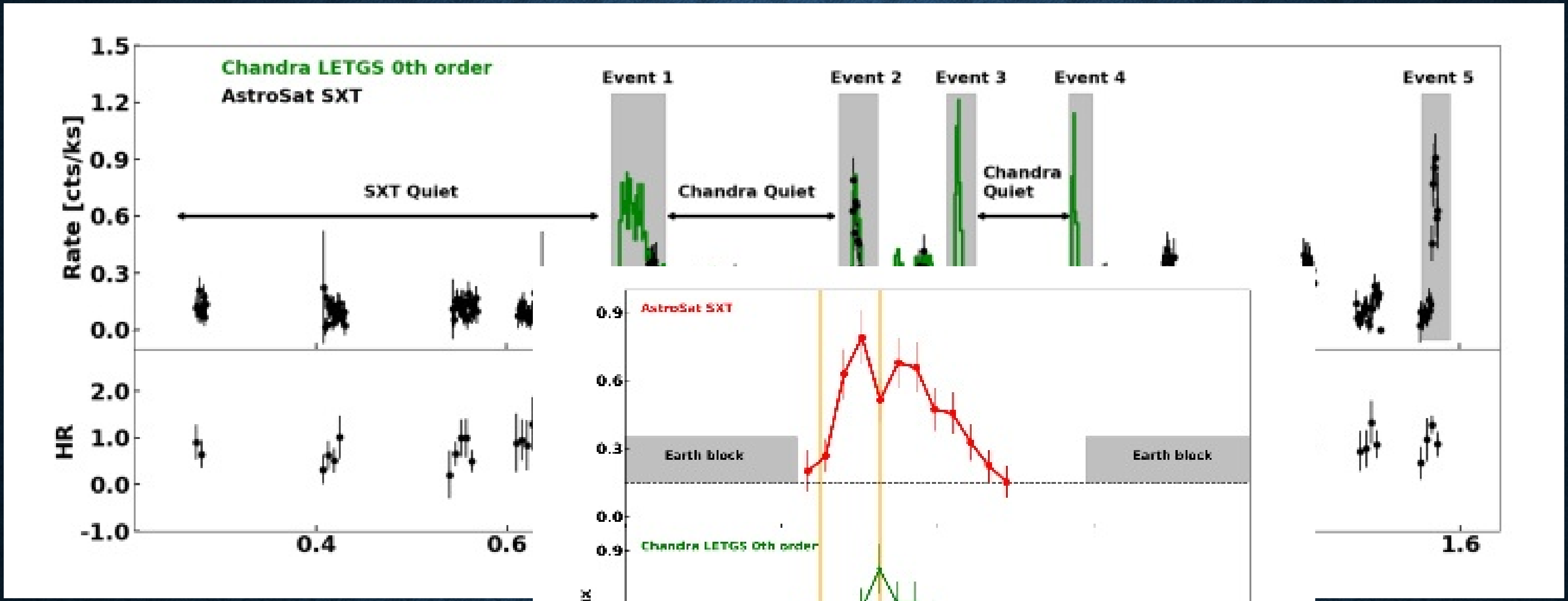

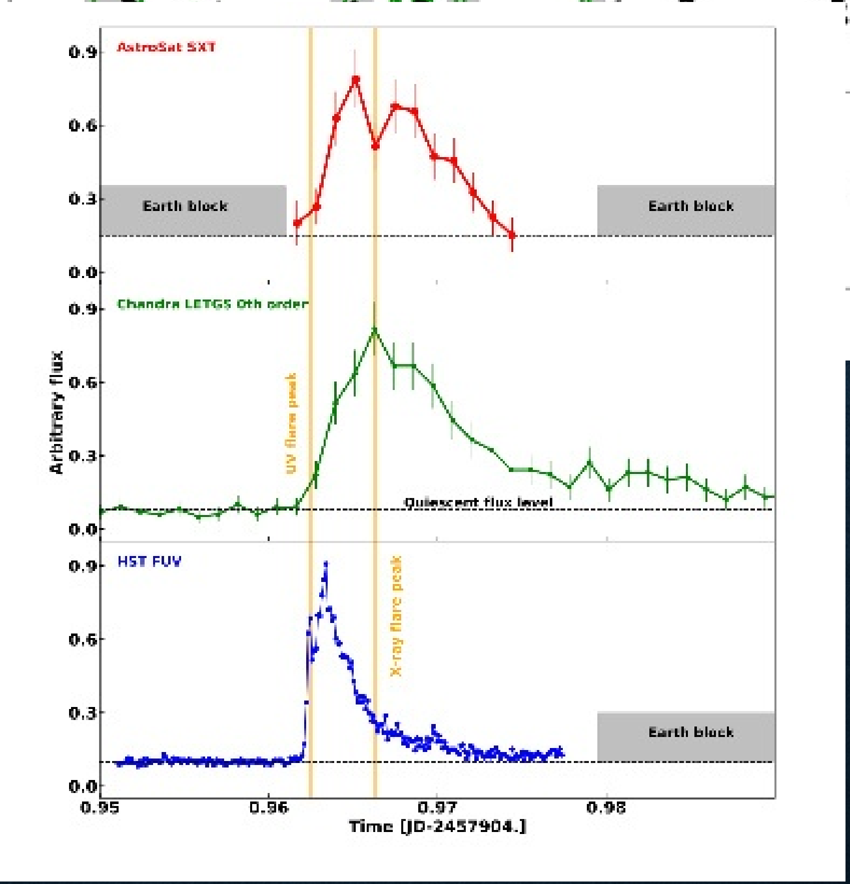

Lalitha et al 2020

DEALING WITH VISIBLE LIGHT LEAKAGE THRU THIN FILTER

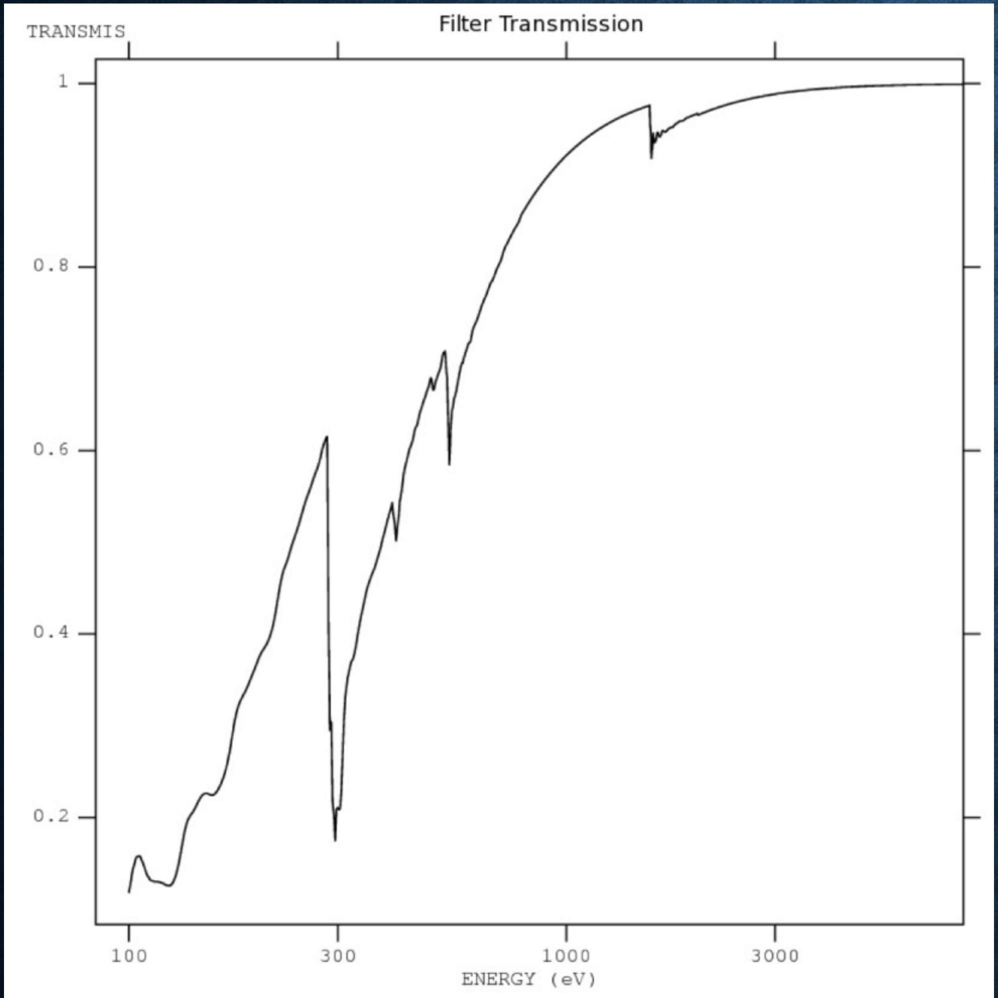

It provides ~7 magnitude of optical extinction over the visible band.

For the Swift XRT with a PSF of ~15” a 6th magnitude star gives an optical loading of a few e- per pixel, at which point the quality of the X-ray data begins to be affected.

For the SXT with a ~7-8 times larger PSF and ~2 times larger angular size of the pixel the safe optical limit is expected to be closer to a ~4th magnitude star,

OBSERVING BRIGHT STARS

Names	HIP 19265	HIP 88580	Capella	HIP 23309
Other Names	HD 24716	HD 165505	αAur	CD-57 1054
Spectral Type	A0	A0	G3 III	M0Ve
B (mag)	8.07	8.05	0.88	11.36
V (mag)	7.94	7.96	0.08	9.98
Distance(pc)	325	226.6	13.1	26.90
Exposure (ks)	9.2	2.0	30.7	18.0

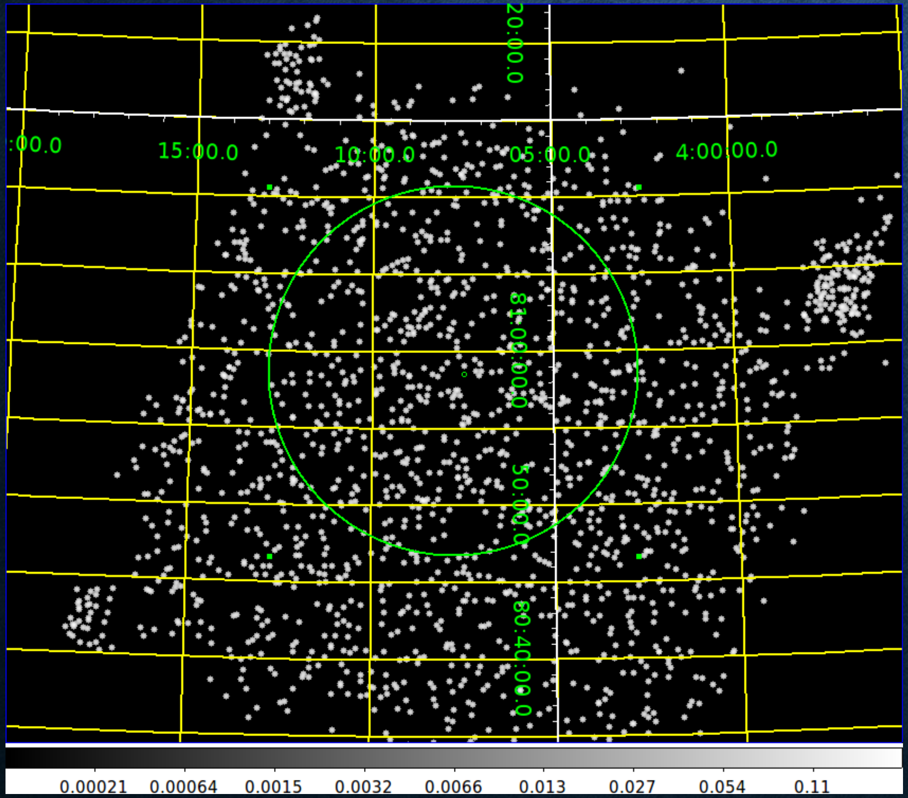

HIP 19265
Event Grades 0-12

Reduced chi^2 = 1.3

OBSERVING BRIGHT STARS

Event Grades 0-12 (left)

Grade 0 only (right)

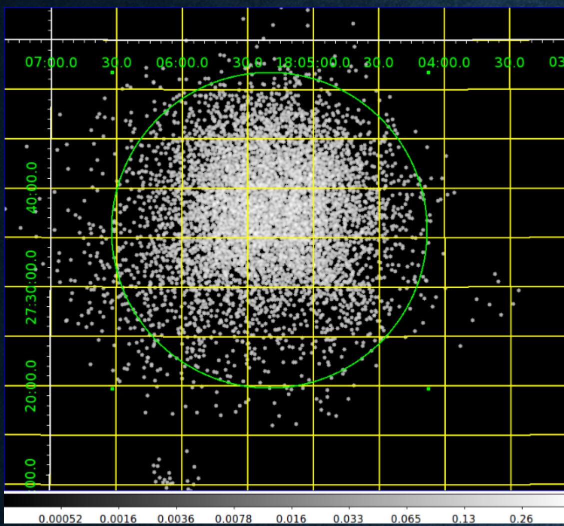

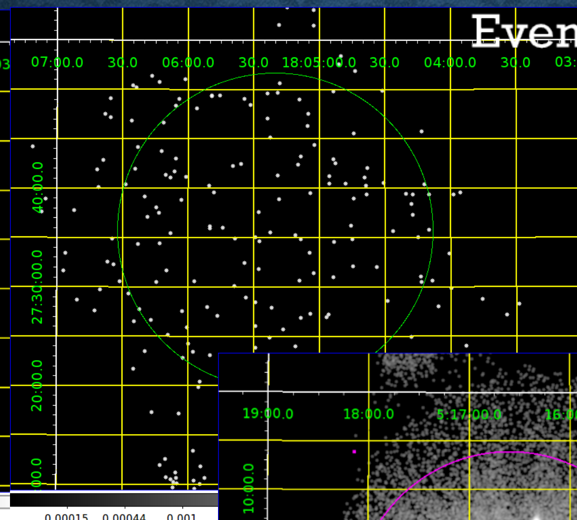

HIP 88580

Capella

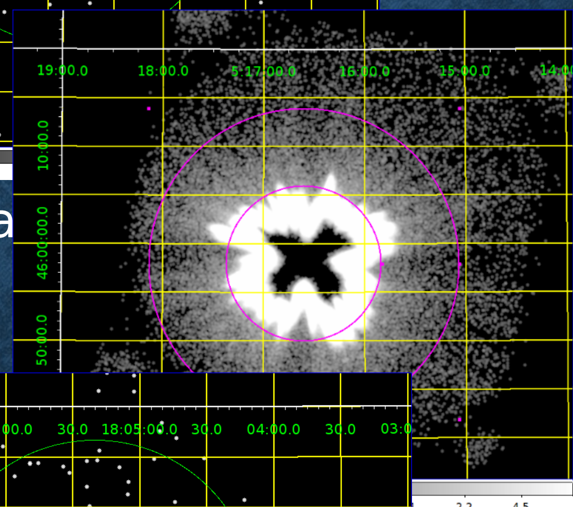

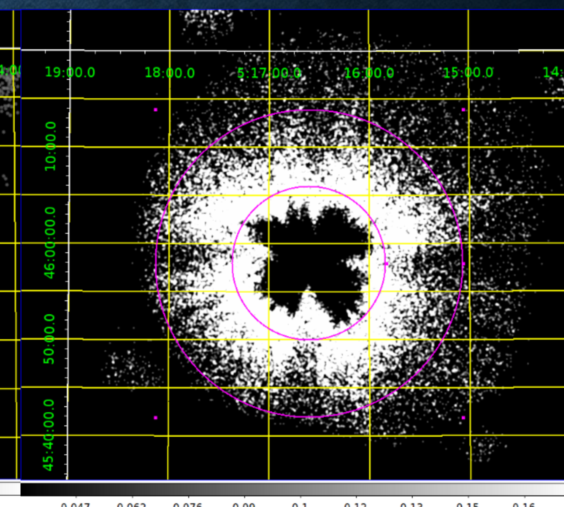

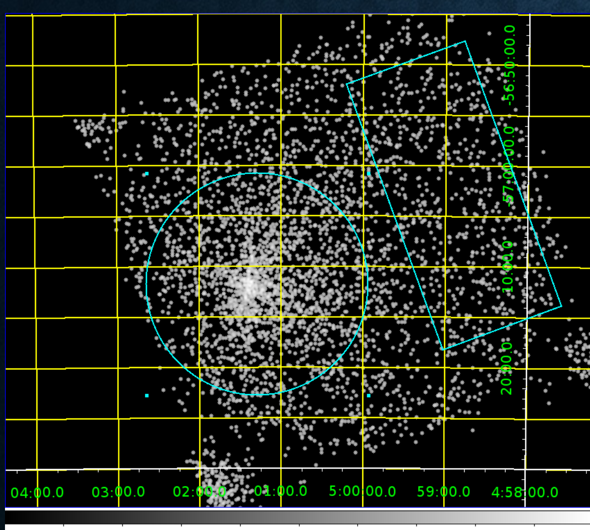

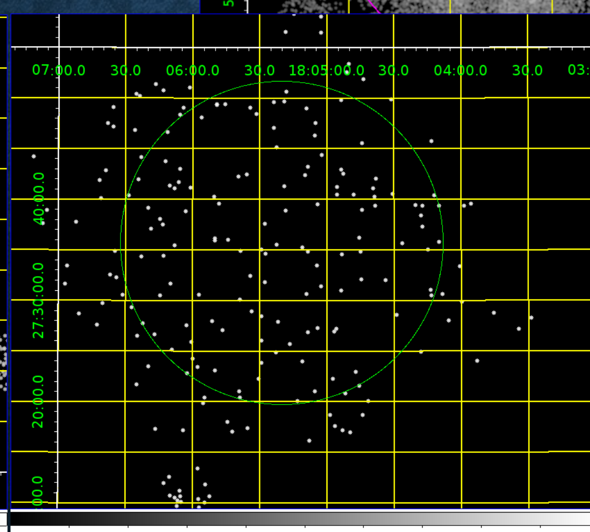

Reduced chi^2 = 1.3

OBSERVING BRIGHT STARS
USE GRADE 0 EVENTS ONLY

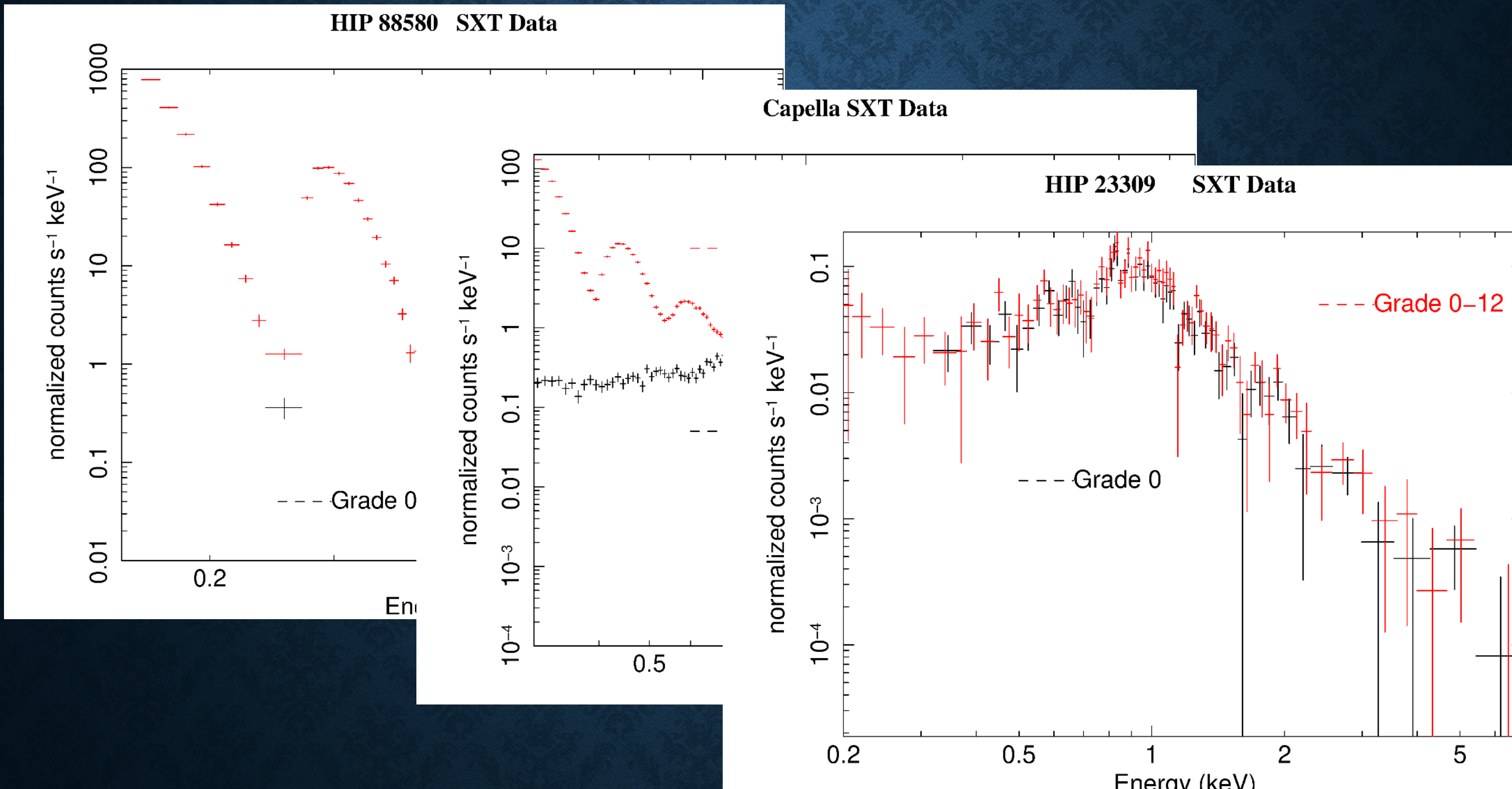

Reduced chi^2 = 1.3

HIP 88580 Capella HIP 23309

THANKS !